Chapter

Seismic Geomorphology, Architecture and Stratigraphy of Volcanoes Buried in Sedimentary Basins

Alan Bischoff, Sverre Planke, Simon Holford and Andrew Nicol

Abstract

Our ability to investigate both the intrusive and extrusive parts of individual volcanoes has evolved with the increasing quality of seismic reflection datasets. Today, new seismic data and methods of seismic interpretation offer a unique opportunity to observe the entire architecture and stratigraphy of volcanic systems, with resolution down to tens of meters. This chapter summarises the methods used to extract the geomorphic aspects and spatio-temporal organisation of volcanic systems buried in sedimentary basins, with emphasis on the utility of 3D seismic reflection volumes. Based on descriptions and interpretations from key localities worldwide, we propose classification of buried volcanoes into three main geomorphic categories: (1) clusters of small-volume (<1 km^3) craters and cones, (2) large (>5 km^3) composite, shield and caldera volcanoes, and (3) voluminous lava fields (>10,000 km^3). Our classification primarily describes the morphology, size and distribution of eruptive centres of buried volcanoes, and is independent of parameters such as the magma composition, tectonic setting, or eruption environment. The close correlation between the morphology of buried and modern volcanoes provides the basis for constructing realistic models for the facies distribution of igneous systems buried in sedimentary strata, establishing the principles for a new discipline of seismic-reflection volcanology.

Keywords: seismic volcanostratigraphy, seismic geomorphology, buried volcanoes, volcanic landforms, igneous plumbing systems, seismic-reflection volcanology

1. Introduction

Subaerial and submarine volcanic landforms originate by primary constructive processes when magma erupts onto the Earth's surface. After the volcanic activity ceases, these volcanic landforms are affected by erosion and weathering, which progressively modify their original morphology. Volcanoes that erupt in environments of relatively high subsidence and low erosion rates can be buried and preserved within sedimentary strata, providing us with an opportunity to investigate the diverse types of volcanic landforms that were formed in the past [1–4].

Volcanic morphologies provide information about the primary and secondary processes that formed them [5–7], and can be used as analogues for understanding buried igneous systems [8, 9]. Our ability to identify buried volcanoes and igneous intrusions emplaced in the shallow (<10 km) layers of the crust has developed immensely over the past four decades in parallel with improvements in the quality and quantity of seismic reflection data. Today, interpretation of seismic reflection datasets indicates that buried volcanoes are characteristic elements of many sedimentary basins globally (e.g. [10–17]).

Seismic interpretation of buried volcanoes benefits from innovations made in the field of sedimentology, in which seismic datasets have been used to analyse in detail the architecture and stratigraphic signature of terrestrial and marine sedimentary systems [18–20]. As noted in [21] *"since the 1960s', attempts to make sense of the diversity of rocks, processes, stratigraphic models and deposition settings of volcanic successions have been aided by major advances in the field of sedimentology"*. Now, seismic reflection data offer unique opportunities to investigate the role of intrusions, host rocks, crustal structures, and relative sea-level variations in the construction and degradation of diverse volcanic landforms [22–24].

Modern seismic reflection datasets allow us to observe the entire architecture of volcanic systems, from the intrusive to the extrusive realms, with resolutions down

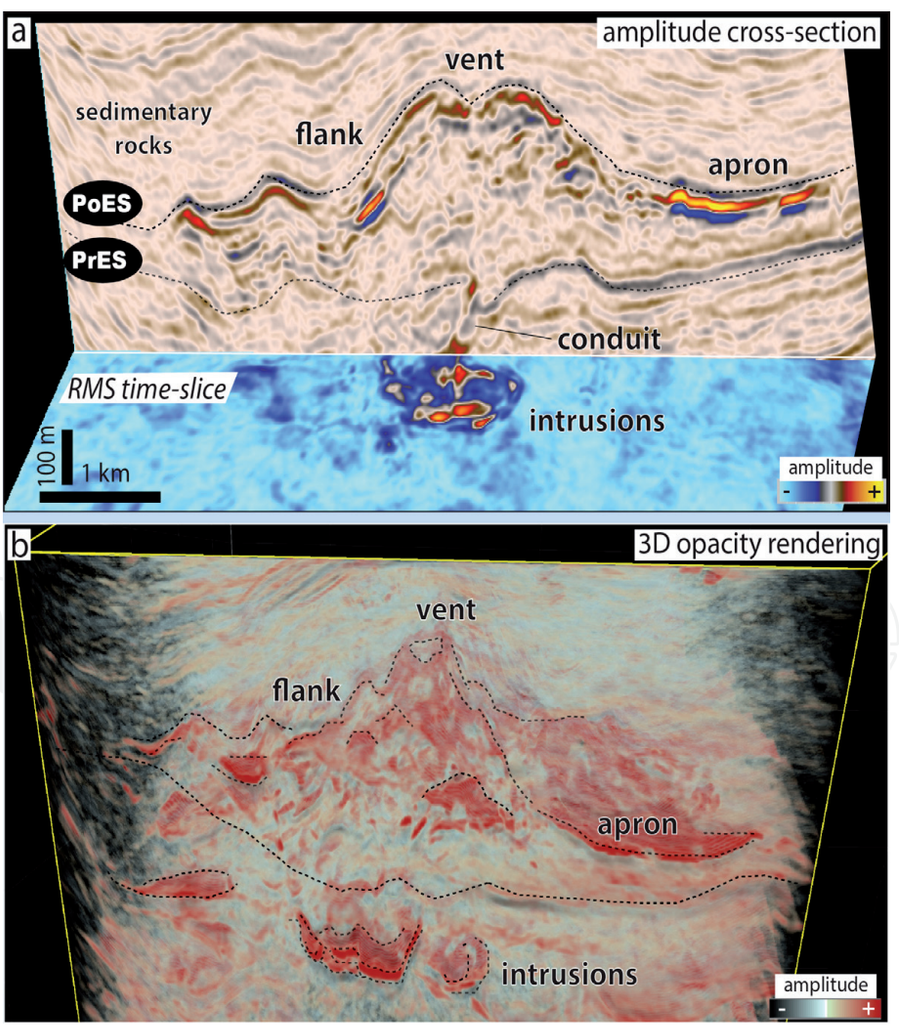

Figure 1.
Seismic reflection visualisation of a small cone-shaped volcano buried in the Taranaki Basin, New Zealand. (a) Shows an amplitude display of a seismic reflection profile across the volcano, coupled with time-slice RMS amplitude display of its plumbing system. (b) 3D opacity-rendered perspective view of the volcano shown in (a) and its shallow (<200 m) plumbing system, in which the low-amplitudes are set as transparent. Note the spatial relationship between the saucer-shaped intrusion and the central vent of the volcano. PrES is the pre-eruptive surface and PoES is the post-eruptive surface.

to tens of metres [25–27]. In particular, new 3D visualisation methods of igneous seismic geomorphology and analysis of volcanic architectural elements have become valuable tools for interpreting buried volcanoes and their impact on the formation and evolution of the host sedimentary basins. The application of 3D visualisation methods leads for direct comparison of the geomorphic aspects of buried volcanoes with modern and ancient outcropping analogues, allowing us to interpret these buried igneous system in great detail [28, 29]. However, the wide variety of volcanic landforms well-documented in volcanic terrains are still not fully assessed in buried volcanic systems.

This chapter highlights the potential for using seismic geomorphology to improve the interpretation of volcanoes buried in sedimentary basins (**Figure 1**). Here, we compare the morphologies of outcropping and buried volcanoes from key localities worldwide. Examples shown in this chapter include description and interpretation of small (<1 km^3) craters and cones, large (>5 km^3) composite, shield and caldera volcanoes, voluminous (>10,000 km^3) lava fields, and subvolcanic sheet-like intrusions. The perceived correlation between the morphology of outcropping and buried volcanoes assist the construction of realistic models from subsurface seismic data, laying the foundations for a new discipline of seismic-reflection volcanology. The information presented in this chapter may have value to geoscientists investigating the impacts of igneous activity on sedimentary basins formation and evolution, and on the processes that control the large-scale (>10^2 m) architecture of volcanic systems on Earth and related planets.

2. Principles of seismic interpretation of igneous rocks

The seismic reflection method is a geophysical technique designed to observe the Earth's subsurface indirectly. This method is based on the recording of artificially generated seismic waves that travel into the Earth's geological formations. At the interface of rock bodies with different physical properties, the waves reflect and refract, producing seismic events with wave amplitudes proportional to the contrast in density and velocity of the rocks that bound the interface [30, 31]. Motion- or pressure-sensitive geophones and hydrophones receivers capture the reflected wavefield from the seismic source. A systematic arrangement of the seismic sources and receivers enables the construction of cross-sections that display images of the Earth's subsurface, with better quality at depths of <10 km [32].

Igneous rocks buried in sedimentary basins are often identified by the presence of anomalously high-amplitude reflections within seismic datasets (**Figures 1** and **2**). Characteristically, dense lavas of basaltic composition and mafic intrusions have compressional (P-wave) velocities >5000 ms^{-1}, contrasting with softer sedimentary rocks which commonly have velocities <3000 ms^{-1} [4, 33, 34]. Despite the straight-forward concept underpinning the identification of igneous rocks based on their high-amplitude reflections, seismic techniques have limitations which leads to uncertainties in the interpretations. Such interpretations are dependent on the quality and resolution of seismic data, which are controlled by geophysical parameters such as wavefield scattering due to changes in rock densities and strata geometries, increasing energy attenuation with depth, and the size of the igneous bodies relative to the wavelength of the seismic signal [35, 36].

Distinguishing buried volcanoes from sedimentary strata can be problematic when the igneous rocks have similar physical properties and geometries as the enclosing host rocks. For example, it may be challenging to differentiate volcanoes from carbonate mounds, or sequences of bedded volcaniclastic and siliciclastic rocks [37, 38]. Secondary alteration processes including mineral changes induced

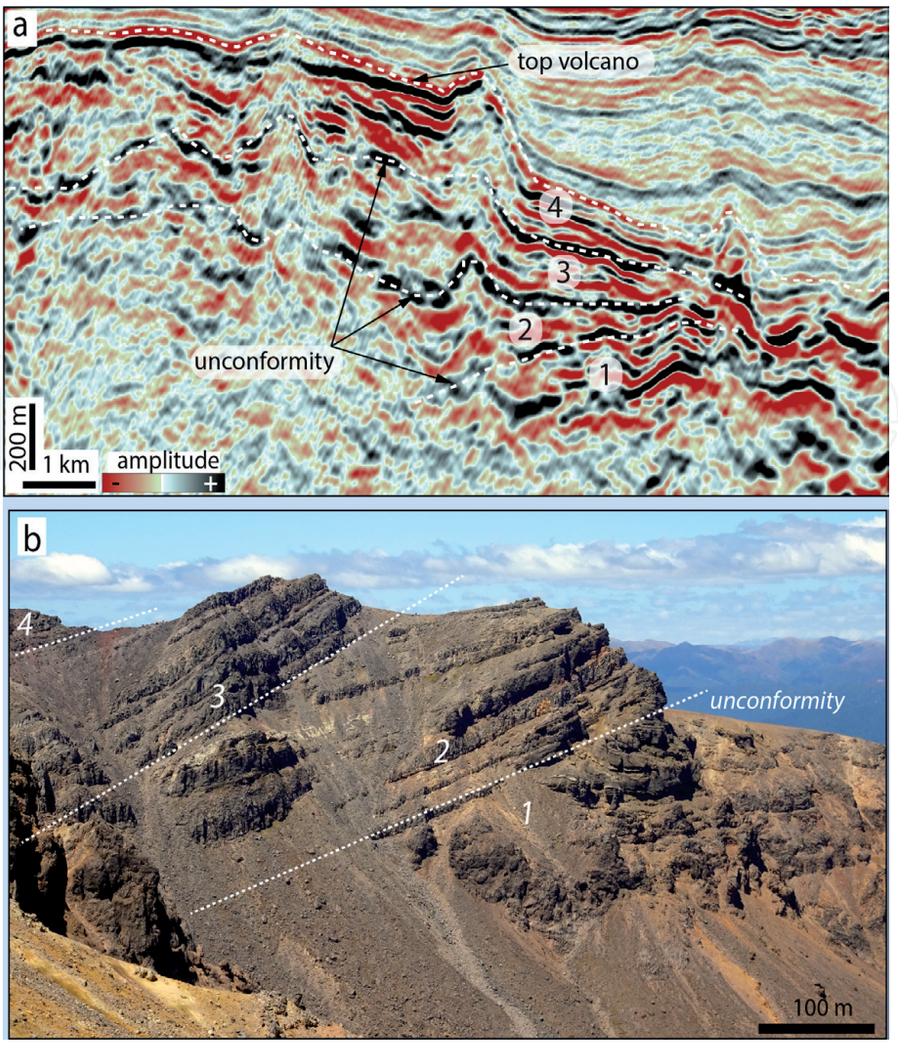

Figure 2.
(a) 2D seismic section across the flank of a polygenetic volcano buried offshore Canterbury Basin, New Zealand. The highest-amplitude seismic reflector in this image marks the interface between the top of the volcanic structure and its overlying sedimentary rocks. (b) Cross-section across an outcropping sequence of lava flows of the Mangahouhounui Fm, Tongariro compound volcano, New Zealand, exposed by erosion. Note that in both seismic and outcropping examples, the relationship between the strata defines a succession of volcanic events bounded by unconformities, across which younger rocks are deposited at the top of the sequence.

by metasomatism and weathering, cementation, compaction during progressive burial, substitution of interstitial pore fluids, and fracturing can also lower the impedance contrast between igneous and sedimentary rocks [39, 40]. In addition, steeply inclined bodies such as dykes and highly heterogeneous subvolcanic zones are often poorly resolved in seismic reflection datasets. These zones can contain numerous intrusive bodies emplaced with variable geometries and spatial relationships to their host strata, leading to loss of reflection coherency [41].

In light of these limitations, seismic interpretation of buried volcanoes can benefit from a fully integrated approach that includes information from drillhole data analysis and insights from modern volcano analogues [42, 43]. In recent years, particular attention has been given to the interpretation of 3D seismic volumes from which cross-sections can be displayed in any given orientation, allowing the visualisation of complex volcanic forms in great detail [44, 45]. This new integrated seismic method, from 2D regional scale to detailed 3D analysis and correlation with drillhole data and analogues, can provide robust interpretations of volcanoes buried within sedimentary basins.

3. Methods and concepts of seismic-reflection volcanology

Interpretation of buried volcanic systems requires a multidisciplinary approach that combines insights from complementary disciplines such as sedimentology, stratigraphy, structural geology, and volcanology into a unified framework. During the last 40 years, our knowledge about the formation and evolution of sedimentary basins has improved mainly due to advances in the fields of seismic and sequence stratigraphy [46–48]. More recently, these stratigraphic approaches have been successfully applied to interpret the processes and products of igneous activity within sedimentary basins [1, 4].

Seismic-reflection volcanology is here defined as the study of buried volcanoes from seismic reflection datasets. This method is typically applied to investigate the nature and evolution of volcanic and igneous plumbing systems buried in sedimentary strata. Sedimentary basins that contain a significant amount of igneous rocks are informally referred to as "volcanic basins" [49–51]. The interpretation of volcanic basins usually begins by mapping the top and base of seismic units (sequences) that are potentially of volcanic origin using 2D regional lines. Mappable seismic facies units are then identified by their distinct aspects in, for example, reflection configuration, continuity, geometry, and interval velocity. A volcanological interpretation is then performed to determine the igneous facies and their intrusive and extrusive enclosing environments. If available, 3D datasets are subsequently interpreted to provide detailed images of the past volcanic surfaces and landforms now buried in the host basin, which is further analysed using the method of igneous seismic geomorphology [29] and volcanic architectural elements [52, 53]. Finally, a more accurate volcanological characterisation of buried igneous rocks can be achieved by correlating the seismic units with data from drillholes and outcrop analogues [26].

The methods used to characterise volcanic basins vary between interpreters and are dependent on the available dataset, scale, and purpose of the study. The following sections summarise these methods focusing on the interpretation of the spatio-temporal expression of buried volcanoes and reconstruction of the scenarios in which volcanic events occurred synchronously with basin sedimentation and erosion.

3.1 Reconstructing the geomorphic aspects, eruptive time, and environment of emplacement of buried volcanic systems

Magma that reaches the Earth's surface can produce a variety of subaerial and subaqueous volcanic landforms. This diversity of volcanic landforms reflects a range of physical factors such as magma composition, discharge rate of effusion, degree of material fragmentation and dispersion, and tectonic and environment settings, in particular, the presence or absence of water where the eruptions occurred [54–57]. In detail, the volcanic landforms are likely the product of many competing processes such as steady versus dynamic mechanisms of fragmentation, fixed versus variable location of the eruptive centre, and single versus multiple eruption phases. Multiple variables can complicate the interpretation of the processes that shaped the geomorphic aspects of volcanoes [6], which is especially true for the characterisation of volcanoes buried in sedimentary strata. In addition to volcanic complexity and limitations of subsurface interpretation, the morphology of buried volcanoes is likely influenced by superimposed post-eruptive processes such as erosion, alteration, compaction, and faulting.

To understand the geological processes that shaped ancient volcanic landforms now buried in sedimentary strata, critical parameters such as the interval acoustic

velocity, and the amount of degradation and compaction of the buried igneous rocks have to be addressed [25]. The height of buried volcanoes is initially inferred from their present-day morphology (i.e. after erosion and compaction during burial) by multiplying the transit time of seismic waves within the volcano by an estimated acoustic velocity of the volcanic interval [58]. The degree of compaction can be estimated by seismic analysis that indicates differential compaction between the volcanic and hosts rocks [59]. Erosional features such as gullies and canyons are typically visible in seismic imagery and can help to evaluate the degree of preservation of the buried volcanic structure [27]. After determining these variables, the morphology of each buried volcanic edifice is approximated as a 3D geometric shape such as a cone, or a spherical cap to roughly estimate their volume. These estimations are "best-fit" approximations which do not affect the first-order (i.e. dimensions of $>10^2$–10^4 meters) interpretations of volcanic morphologies [60].

To make sense of this seismic morphological information, the interpreter of volcanic basins typically construct volcanostratigraphic frameworks that help to explain the succession of igneous and sedimentary events occurred during the evolution of the basin (**Figure 3**). The age of the volcanic rocks in the subsurface is commonly determined by correlating seismic isochron horizons with biostratigraphic markers and radiometric dating of rocks penetrated by nearby drillholes. This approach gives time resolution in the order of 0.1 to 5 Myr, assuming that the seismic reflections provide a proxy of timelines [48, 61]. Interpretation of the environment in which the buried volcanoes erupted can be determined by seismic

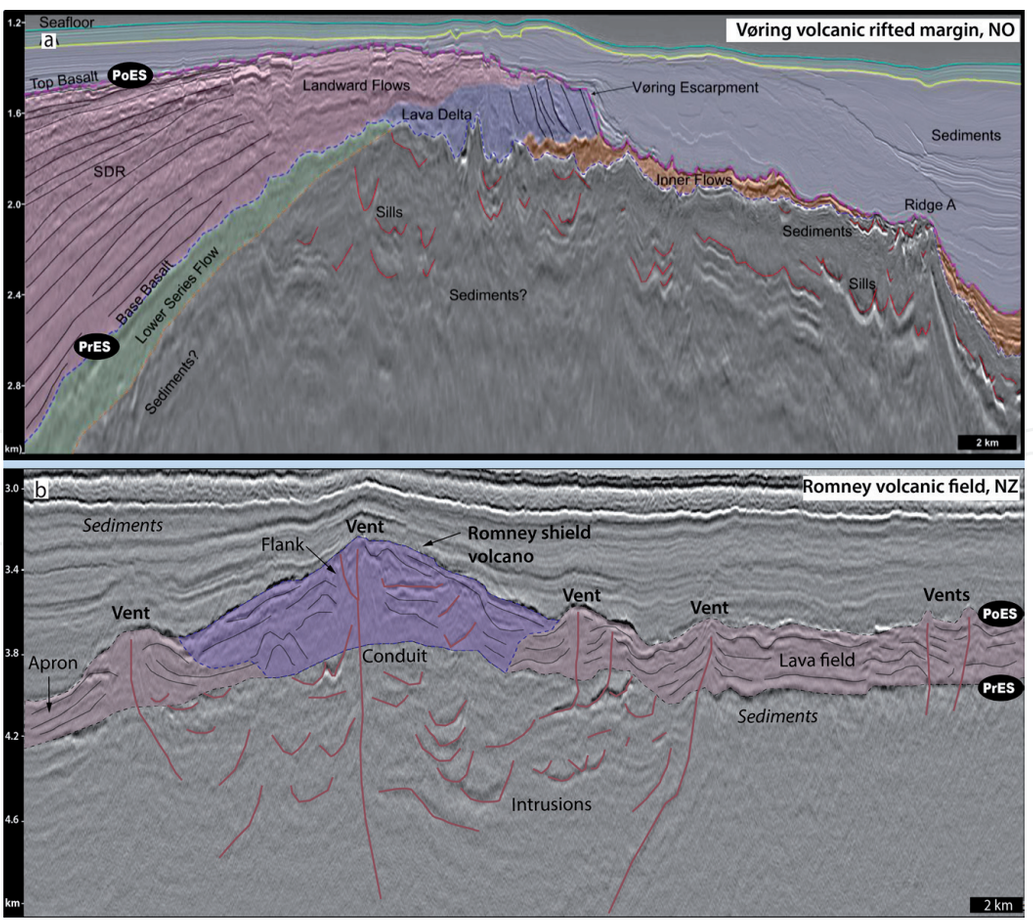

Figure 3.
Amplitude display of seismic reflection profiles across the Vøring volcanic rifted margin, offshore Norway (a) and the Romney volcanic field, offshore New Zealand (b). Note that the internal and external configuration of seismic reflections determines the spatial relationship of distinctive seismic units, providing information about the succession of events that have formed these units. Data courtesy of TGS (a) and NZPAM (b).

stratigraphic analysis calibrated with paleoenvironmental data obtained from microfossils from drillholes across the studied areas or correlative outcrops [62]. As standard procedure in the analysis of seismic datasets, 2D sections and 3D perspective views are often displayed with vertical exaggeration to enhance the stratal relationship of seismic reflections, which modify the visual geometric aspect of the buried volcanic landforms.

3.2 Seismic volcanostratigraphy

Seismic volcanostratigraphy is a subset of the seismic stratigraphic method developed to analyse the geological evolution and environments of emplacement of igneous extrusive rocks using seismic reflection datasets [4]. This method consists of two main steps: (1) mapping of the top and base of volcanic sequences, and (2) seismic facies analysis, including characterisation of volcanic and enclosing sedimentary seismic facies units and their volcanological interpretation (**Figure 3**).

The application of seismic volcanostratigraphy relies on the identification of changes in basin depositional trends, placing stratigraphic boundaries at the contacts between volcanic units that are genetically related [1, 29, 63]. In non-volcanic basins, such trends represent the dispersal and accommodation of material in specific stacking patterns of progradation, retrogradation and aggradation. These depositional trends reflect oscillations of the base level that result in erosion and accumulation of sediments within the basin, which is typically controlled by the balance between variables such as tectonics, eustasy, and climate [64, 65].

Igneous activity can strongly impact the depositional trends of sedimentary basins, which requires adaption when using conventional stratigraphic concepts and nomenclature for stratigraphic interpretation of volcanic sequences (**Figure 4**). For example, the stratal trends of non-volcanic basins are typically described according to variations in the position of the shoreline through time [66]; while in volcanic

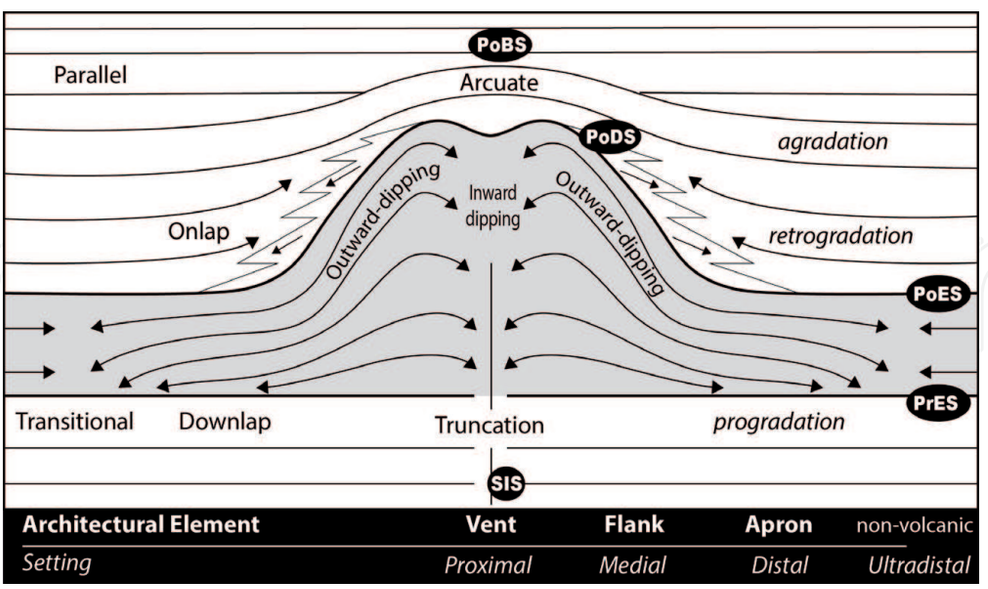

Figure 4.
Simplified representation of the main stratal patterns, volcanic architecture, and depositional settings of cone-shaped volcanoes buried in sedimentary strata. The arrows indicate the patterns of material dispersal in specific stacking patterns of progradation, retrogradation and aggradation. The geometric configuration of strata reflects the interplay between volcanic and sedimentary processes experienced during the evolution of the basin. Note that the eruptive centre is the focal point that determines the spatial relationships between proximal to ultradistal depositional settings, which can be used as a model to predict how volcanic and sedimentary lithofacies may be distributed within and around the volcano. SIS: syn-intrusive surface. PrES: pre-eruptive surface. PoES: post-eruptive surface. PoDS: post-degradational surface. PoBs: post-burial surface. See [53] for detailed information of these volcano stratigraphic surfaces.

systems, the focal point for discussing stratal trends is the eruptive centre [8, 52]. This is because the addition of material sourced by eruptions and isostatic adjustments of the crust caused by magma emplaced in the subsurface can overprint normal basin processes such as sediment supply and the available accommodation space [67, 68]. As a consequence, igneous activity can have a major control on the basis stratal trends, possibly impacting the architecture and evolution of the basin over thousands of square kilometres and for millions of years (**Figures 3** and **5**).

Volcanic activity often causes sudden changes in basin stratal patterns, which make it relatively straight-forward to identify the large-scale unconformities that mark the boundaries of entire volcanic sequences [45]. A typical volcanic sequence initiates with a progradational or aggradational trend marked by truncations and downlaps onto the pre-eruptive surface, and it ends with a retrogradation trend visible by onlap terminations on the top of the post-eruptive surface [4, 52]. Internal unconformities and trends within the volcanic sequence are more subtle than large regional unconformities, and may only be identified in high-quality 3D datasets (**Figure 2**). The identification of volcanic stratal patterns can be complicated due to rapid and in some cases cyclical switches from constructional to degradational stages of polygenetic volcanoes, making it challenging to map the lateral extension of volcanic unconformities [69, 70].

In some circumstances, the reduced seismic quality below thick volcanic sequences can difficult the identification of the pre-eruptive surface [35]. Similarly, the post-eruptive surface is not always marked by onlap of overlying strata onto a volcanic structure, which depends on the interplay between the rate of material sourced by eruptions versus the rate at which the volcano has been buried by sediments sourced from other parts of the basin [52]. In other words, onlap onto an active volcanic edifice can occur if the rate of burial overcomes the rate and volume of erupted material, which may be expected during the later stages of long-lived volcanoes, especially if the eruptions do not form layers thick enough to be resolved in seismic data (**Figures 4** and **5**). Additional stratigraphic markers such as the syn-intrusive, post-degradational and post-burial surfaces help to constrain the impacts of igneous activity in the host basin into a spatio-temporal framework [53].

3.3 Igneous seismic facies units

Buried volcanic systems often show distinctive seismic facies units that result from the interaction of igneous activity and its surrounding sedimentary host rocks and

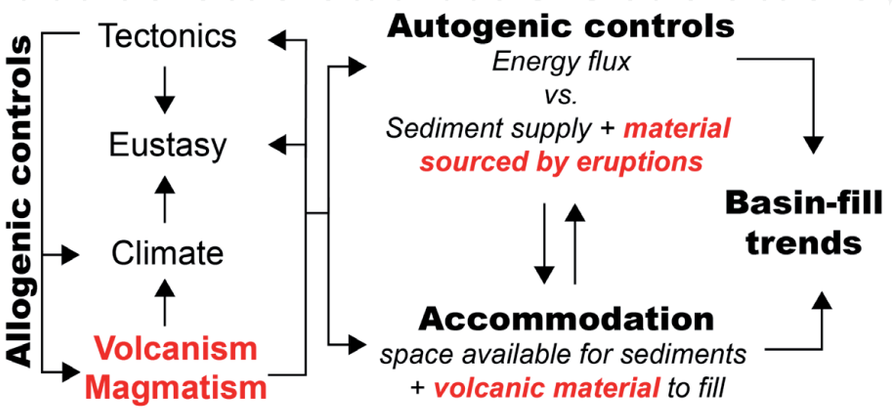

Figure 5.
Processes that control the stratigraphic signature and architecture of sedimentary basins impacted by igneous activity. The interplay of competing autogenic (i.e. from within the system) and allogenic (i.e. from outside of the system) mechanisms defines the depositional trends of volcanic basins. Adapted from [66].

environments. Seismic facies analysis consists of mapping of 3D units and 2D profiles whose seismic parameters differ from those of adjacent units [71], followed by a volcanological interpretation of the mapped seismic facies units [3]. Discrete seismic reflection packages often correspond to depositional units that are genetically related and bounded by seismic discontinuities (**Figure 2**). Variations in igneous seismic facies represent changes in the volcanic processes and environments that enclose the buried volcanoes (**Figure 6**). These seismic facies units can be interpreted in terms of volcanic eruptions, magma emplacement mechanisms, and sedimentation patterns developed during the evolution of the host sedimentary basin [4, 22, 73].

Seismic attribute analysis such as coherency, amplitude, frequency, and attenuation (or a combination of these) can be used to enhance the contrasts between variations in the physical properties of the buried igneous rocks units and their

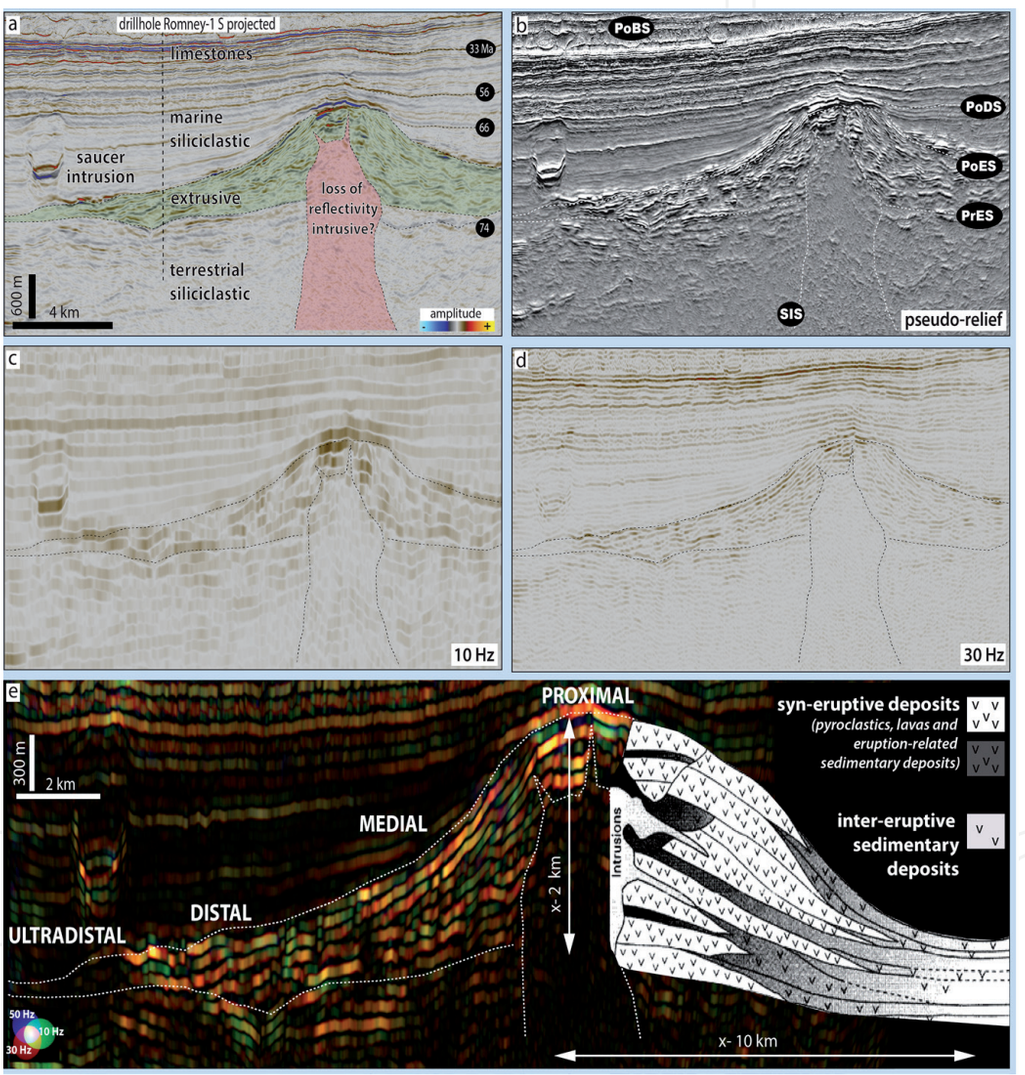

Figure 6.
(a) Amplitude display of a seismic reflection profile across Vulcan composite volcano, offshore Deepwater Taranaki Basin, New Zealand, illustrating a variety of intrusive, extrusive and sedimentary seismic facies. The age and lithofacies and their correspondent seismic facies are calibrated with information from the Romney-1 petroleum exploration well, located 50 km north of Vulcan volcano. Approximate ages of the chronostratigraphic surfaces are shown in the back circles. Note how igneous and limestone rocks tend to form the highest amplitude events in this cross-section. The low reflectivity seismic facies below the volcanic edifice are often present in subvolcanic zones. (b) Pseudo-relief and amplitude displays (c and d) seismic profiles across Vulcan volcano. These seismic attributes highlight the differences between igneous and sedimentary rocks. The increase in the frequency of the seismic signal (10–30 Hz) highlights the internal structure of the volcano. (e) Spectral-decomposition display of a seismic reflection profile across Vulcan volcano illustrating the idealised facies architecture of large polygenetic volcanoes. The schematic facies diagram is adapted from [67]. X- corresponds to the average diameter and height of composite volcanoes, based on [72].

enclosing sedimentary strata (**Figure 7**) [30]. More recently, the use of machine learning techniques and artificial neural networks have been applied to delineate igneous seismic facies [74]. Description of igneous seismic units can be used to interpret volcanic landforms and different parts of volcanic systems. For example, cone-type volcanoes such as cinder cones and stratovolcanoes typically display a pair of inward- and outward-dipping reflections that mark the location of a central crater and peripheral flanks. Optimal characterisation of buried volcanoes can be obtained by analysing the igneous seismic facies as part of a genetically related network in different scales of observation, which consist in mapping intrusive and extrusive igneous seismic units into a unified interpretation framework [29, 52, 73].

3.4 Igneous seismic geomorphology

Seismic geomorphology is the application of analytical techniques to study ancient buried sedimentary systems imaged by 3D seismic data [18, 20, 75]. Similarly, igneous seismic geomorphology analyses the 3D characteristics of buried volcanoes and shallow crustal intrusions from a geomorphological perspective [29]. This technique is based on the extraction of horizons and slices from the seismic volume at scales and geometries comparable to modern volcanic morphologies (**Figures 1** and **6**). A variety of analytical techniques, such as opacity rendering, spectral decomposition, iso-proportional slicing, and mapping of geobodies can be applied to image the geometric aspects, spatio-temporal distribution and relationship of seismic units [76].

When integrated with seismic and sequence stratigraphy, seismic geomorphology provides background information to interpret the morphology and architecture of buried volcanoes (**Figure 7**). In outcrop, the morphological characteristics of volcanoes provide insights into past eruptive styles, edifice growth mechanisms, and

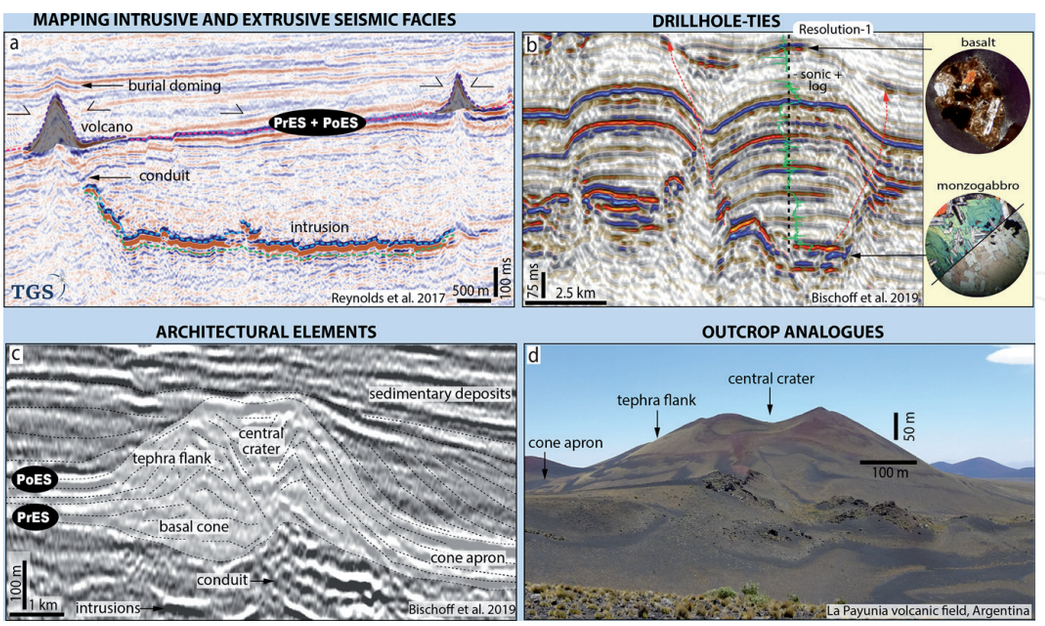

Figure 7.
Examples of techniques used to recognise igneous rocks buried in sedimentary basis. (a) Amplitude seismic section displaying typical saucer-shape sill and related vents located above the termination of the sill, Bight Basin, southern Australia. From Reynolds et al. [15]. (b) 2D seismic cross-section showing a monzogabbro intrusion and associated volcanogenic deposits, tied to lithologies penetrated by the Resolution-1 exploration drillhole, Canterbury Basin, New Zealand. From Bischoff et al. [22, 37, 53]. (c) 2D amplitude seismic cross-section illustrating the main architectural elements of a small mound-shaped volcano buried in the Canterbury Basin, New Zealand. From Bischoff et al. [22, 37, 53]. (d) Photograph illustrating the main architectural elements of a Holocene cinder cone in the La Payunia volcanic field, Argentina. Note the similar morphology of volcanoes in seismic imagery and modern outcropping analogues.

cone degradation experienced during their complete history [21, 77]. Correlating the morphological aspects of buried and outcropping volcanoes can assist in developing the best possible model for the volcanic emplacement in its surrounding environments, including prediction of lithologies, stratigraphic architecture, and geological processes occurred during their evolution (**Figures 6** and 7).

3.5 Architectural elements of buried volcanoes

The concept of architectural elements was introduced to sedimentary geology during the 1980s' and 1990s' to document the fundamental building blocks of fluvial and deep-water systems [20, 78, 79]. The systematic documentation of the variety and arrangement of architectural elements such as channels, levees, and accretionary bars are critical for the interpretation of buried sedimentary environments, with particular relevance to the 3D interpretation of seismic reflection datasets [80].

An architectural element is defined as a three-dimensional genetically related rock unit characterised by its geometry, facies, composition, scale, and bounding-surfaces, and is the product of a particular process or suite of processes occurring within a depositional system [81]. The architectural elements approach investigates the internal arrangement and external bounding-surfaces that delimit co-genetic lithofacies and seismic units [47]. These elements are typically described at a scale of macroforms (i.e. bedforms with lengths of 10^2–10^4 meters), using [82] terminology.

Volcanic landforms including their small-scale variants such as basaltic monogenetic cinder cones and maar-diatreme volcanoes also comprise a combination of particular building blocks with scales comparable to those of sedimentary macroforms. For example, cinder cones typically display a central crater with marginal tephra flanks, while a maar volcano characteristically has a diatreme circled by a tephra ring [6, 83]. Each of these fundamental volcanic building blocks (i.e. architectural elements) are often >100 m in horizontal and vertical dimensions [72], therefore, they may be recognisable in seismic reflection datasets (**Figures 6** and 7).

Facies models of modern and ancient outcropping volcanoes show a systematic variation of macroforms and lithofacies, which are typically spatially distributed according to their distance from eruptive centres [21, 67, 84]. Comparing the variety and arrangement of buried architectural elements with volcanic facies models available in the literature helps us to predict the three-dimensional patterns of igneous and sedimentary lithofacies within buried volcanic systems (**Figures 4, 6** and 7). This information can then be used to assist the interpretation of the geological processes that formed the volcanoes now buried in the subsurface [52, 53].

4. Morphology and architecture of buried volcanic systems

4.1 Shallow subvolcanic intrusions

The majority of melt generated by igneous activity likely fails to reach the Earth's surface [85]. Within sedimentary basins, magma often forms widespread plumbing networks that can extend laterally for tens of kilometres before it erupts [43]. The movement of magma through the shallow layers of the crust and its interaction with heterogeneous host rocks and faults are primary parameters that constrain the geometries of intrusive bodies and the location of eruptive centres [86–88].

Volcanic plumbing systems emplaced in sedimentary strata comprise numerous intrusive bodies of various shapes and sizes. These bodies are broadly classified into

sheet-like intrusions such as dykes, sills and cone sheets, and more massive equidimensional forms, including laccoliths, plugs, and plutons [24, 89, 90]. Sheet-like intrusions prevail in sedimentary basins because magma tends to propagate through and along with weakness plans of the host strata and faults. Dykes are understood to be the main vertical pathways for magma feeding eruptive centres [91], while sills mostly distribute melts laterally across the basin [92]. This is because, by definition, sills are dominantly parallel with the usual sub-horizontal basin strata (including layers of lava or sedimentary rocks), whilst dykes dominantly cross-cut layering in basin host rocks.

However, magmatic intrusions may extend for tens to hundreds of kilometres [93–95], limiting our ability to observe their complete geometry exclusively from outcrops. Seismic reflection profiles can provide large scale images (tens to hundreds of km's) of entire intrusive bodies, allowing us to describe their geometric aspects, lateral and vertical dimension, and interconnectivity in detail (**Figure 8**). Interpretation of seismic data from volcanic basins has revealed that sills can locally display geometries that are discordant with the host rocks. These discordant sills are described in terms of their geometry in relation to the orientation of the host strata, comprising morphologies such as transgressive, step-wise, and saucer- and v-shaped sills [59, 96]. This improved understanding of the migration of magma through interconnected intrusions demonstrated the critical role of sills in transferring

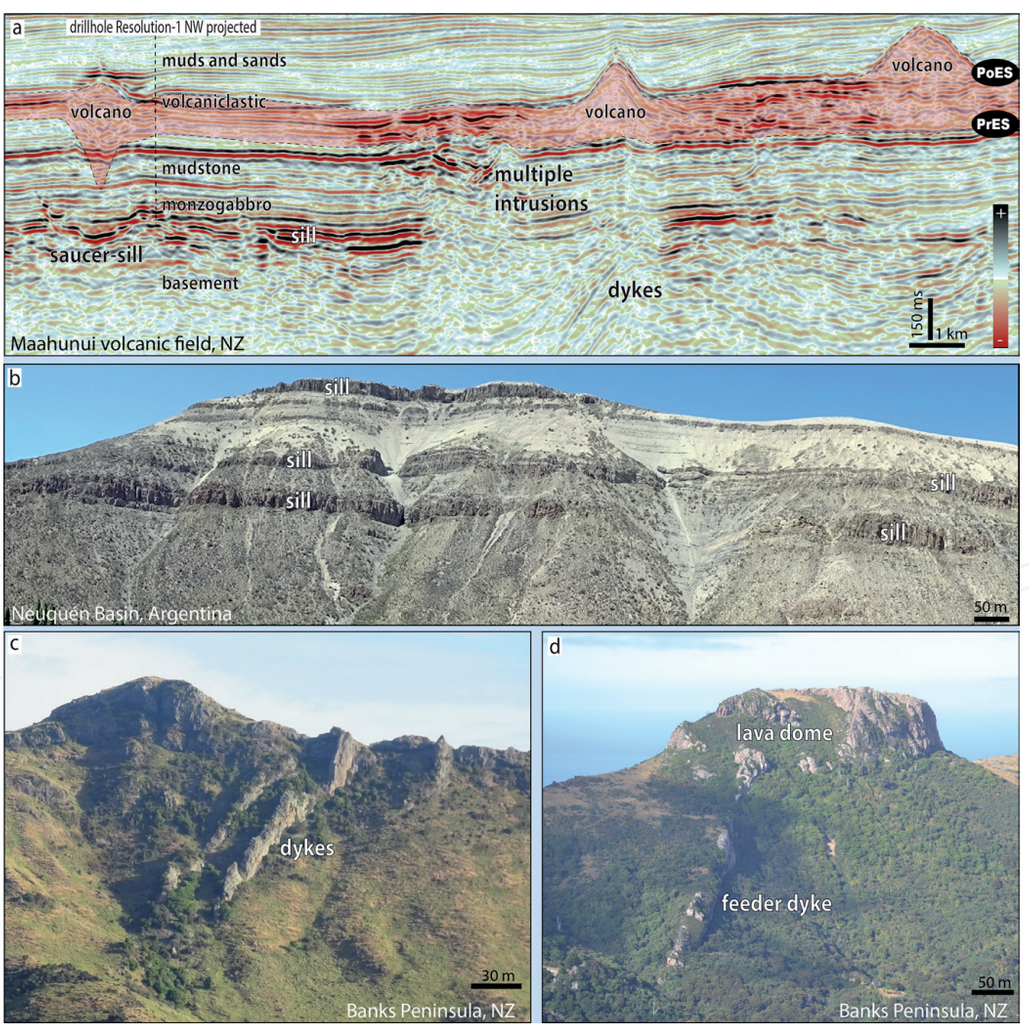

Figure 8.
Seismic examples and outcrop analogues of tabular sills and dykes. (a) Amplitude seismic display across small vents and shallow correlative intrusions of the Maahunui volcanic field, offshore New Zealand [22]. (b) A series of extensive flat-lying sills emplaced parallel to marine strata of the Neuquén Basin, Argentina. (c and d) Sub-vertical dykes cross-cutting a sequence of lava and pyroclastic flows of the Banks Peninsula compound volcano, New Zealand.

magma from depths to upper layers of the crust, which has been reinforced by observations from laboratory experiments [89, 97].

Numerous sills in sedimentary basins have a saucer-shaped geometry consisting of a flat-lying inner sill connected to outer inclined sheets (**Figure 9**). Saucer-shaped sills are usually (but not always) identified in 2D seismic lines by a concave-upward high-amplitude reflection located below an anticlinal fold, suggesting that emplacement of the sill uplifted the overlying strata [98]. Reflections displaying onlap terminations on the top of these folds typically indicate the timing of intrusion emplacement [99]. The upper termination of the inclined sheets is often associated with small craters and cones that erupted at the paleosurface, suggesting a relationship between saucer-sills and vent complexes (**Figure 6a**). The vent complexes can be of both hydrothermal (phreatic) and magmatic origin [58–60].

Dykes and other thin (<50 m) sub-vertical intrusions (i.e. conduits) can be inferred using principles from fault interpretation, by the presence of narrow and sub-vertical bright discontinuities associated with disrupted enclosing reflections [52, 100]. The application of this disrupted-reflector criteria for dyke identification is more likely to be accurate if the sub-vertical discontinuities are located below a vent zone or related to flat-lying intrusions. Dike swarms have been interpreted by steeply inclined high-to-moderate amplitude reflections cross-cutting sedimentary strata in offshore Norway [101] and New Zealand (**Figure 8a**).

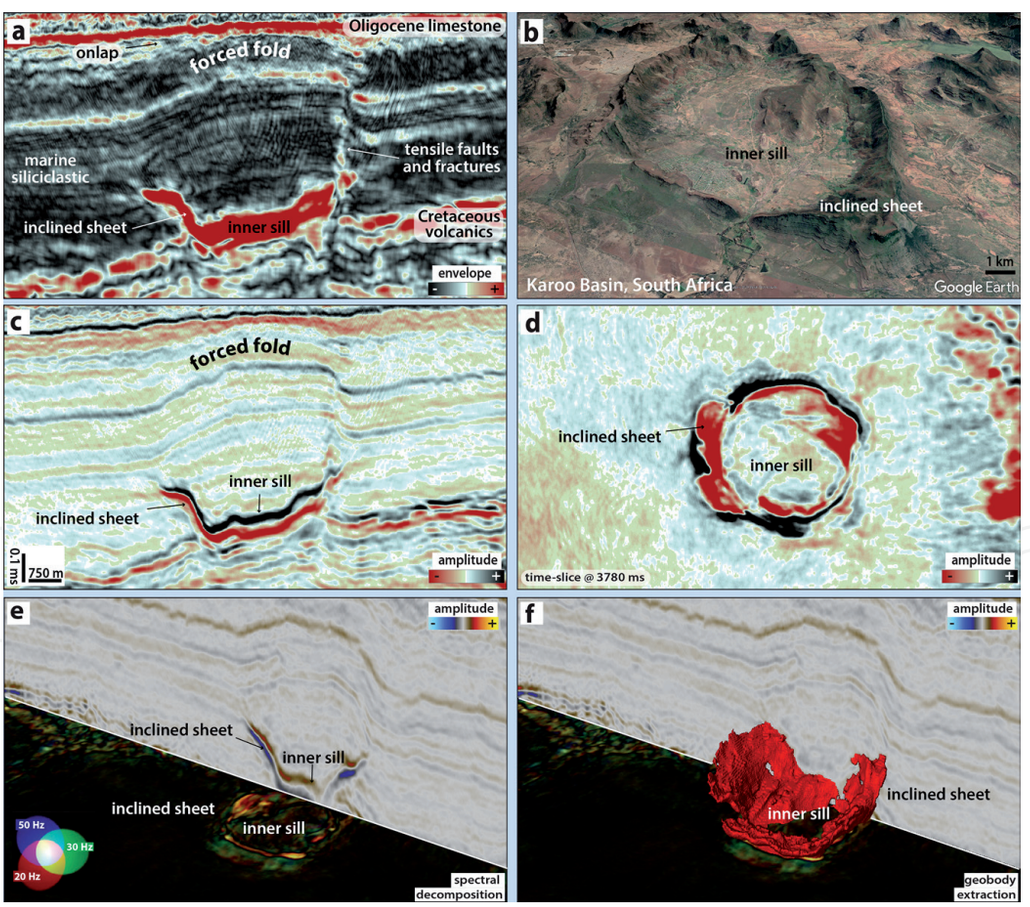

Figure 9.
Seismic and outcrop examples showing the typical geometry of saucer-shaped intrusions. (a) Envelope display across a saucer-intrusion of Eocene age emplaced in Cretaceous to Paleocene strata of the Deepwater Taranaki Basin, New Zealand. (b) Saucer-intrusion emplaced in sedimentary strata of the Karoo Basin, South Africa. Cross-section (c) and in plain view (d) amplitude display of the intrusion shown in (a). (e) Composite 3D perspective display of an amplitude cross-section and a time-slice of a spectrally decomposed seismic cube across the intrusion in (a). (f) Same view as (e) extracting the seismic geobody that corresponds to the 3D geometry of the intrusion. This hybrid intrusion comprises an inner sill parallel to the sedimentary strata, and peripheral inclined sheets cross-cutting the host strata.

4.2 Clusters of small-volume craters and cones

Clusters of discrete, small-volume (i.e. <1 km^3) craters and cones occur in most tectonic settings around the world. These clusters often contain tens to hundreds of volcanoes associated with rifting (e.g. Assab Volcanic Field, Ethiopia), intraplate volcanism (Newer Volcanic Province, Australia) and subduction zones (Pinacate Volcanic Field, Mexico). Typically, they comprise basaltic monogenetic volcanoes such as scoria cones, tuff rings, maars-diatremes, and hydrothermal vents, although some examples can also be of dacitic, phonolithic, trachytic, and rhyolitic composition [72, 102]. The basaltic fields are commonly derived from mantle melts with minor fractional crystallisation and little crustal assimilation, sourcing low-viscosity magmas that can feed widespread lava-flow fields adjacent to the craters and cones [103]. Clusters of dacitic to rhyolitic lava domes and explosive vents are rare and more commonly erupted as the final events of large silicic caldera-forming cycles, or from their associated fissures systems [104, 105].

The primary morphology of small craters and cones can display simple or complex geometries, which are determined by parameters such as the content of volatiles dissolved in the magma and water-melt interactions in the environment surrounding the eruption [83, 106]. Small mafic volcanoes dominated by a mound- or conical-shaped geometry (i.e. spatter, scoria, and tuff cones) are often constructed by accumulation of fragmental volcanic material (tephra) ejected by relatively low-energy pyroclastic eruptions such as fire-fountaining, Strombolian and Vulcanian eruptive styles (**Figure 10a**-**d**). Although each mound-shaped volcano presents characteristic morphometric forms, their simpler end-members all share a systematic distribution of macroforms in relation to the vent zone. This typical macroform distribution comprises of a proximal central crater circled by peripheral flanks that are enclosed by a distal tephra (or lava field) apron [6]. Average sizes of cone-shaped volcanoes are ca 300 m height and 1 km basal width, with spatter cones having the smallest dimensions and tuff cones the largest sizes [72]. By contrast, small volcanoes dominated by a crater-shaped geometry (i.e. tuff rings and maar-diatremes) typically result from phreatomagmatic eruptions (including Surtseyan styles) triggered by molten-fuel-coolant interactions of magma, water, CO_2, and thermogenic gases [107, 108]. These volcanoes have craters up to 3 km in width and maximum depth up to 500 m. The distribution of macroforms in a tuff ring consists of a central crater circled by a peripheral ejecta ring and a debris apron [109], while Maar-diatremes display a root zone, a lower unbedded and upper bedded diatreme, an ejecta ring, and an associated debris apron (**Figure 10e**-**h**).

The seismic expression of small craters and cones are comparable to geometries observed in outcropping volcanoes [9, 27]. In seismic cross-sections, mound-shaped volcanoes are inferred from mounds that built-up above a relatively flat pre-eruptive surface. Chaotic or inward-dipping reflections at the centre of the mounds suggest the location of the vent zone, while lateral inclined, parallel, continuous or disrupted outward-dipping reflections indicate the position of the flanks (**Figure 10a**-**d**). The mounds may or may not contain peripheral sub-horizontal continuous to discontinuous high-amplitude reflections that represent lava-flow fields and tephra aprons. In contrast, the crater-shaped volcanoes show V-shaped excavations into the pre-eruptive surface. These craters typically contain unbedded, disrupted and chaotic reflections at the base (i.e. lower diatreme), and discontinuous to bedded reflections at the top (upper diatreme). The crater-shaped volcanoes are often circled by moderate to high-amplitude reflections that likely represent material ejected by large pyroclastic eruptions [2, 53].

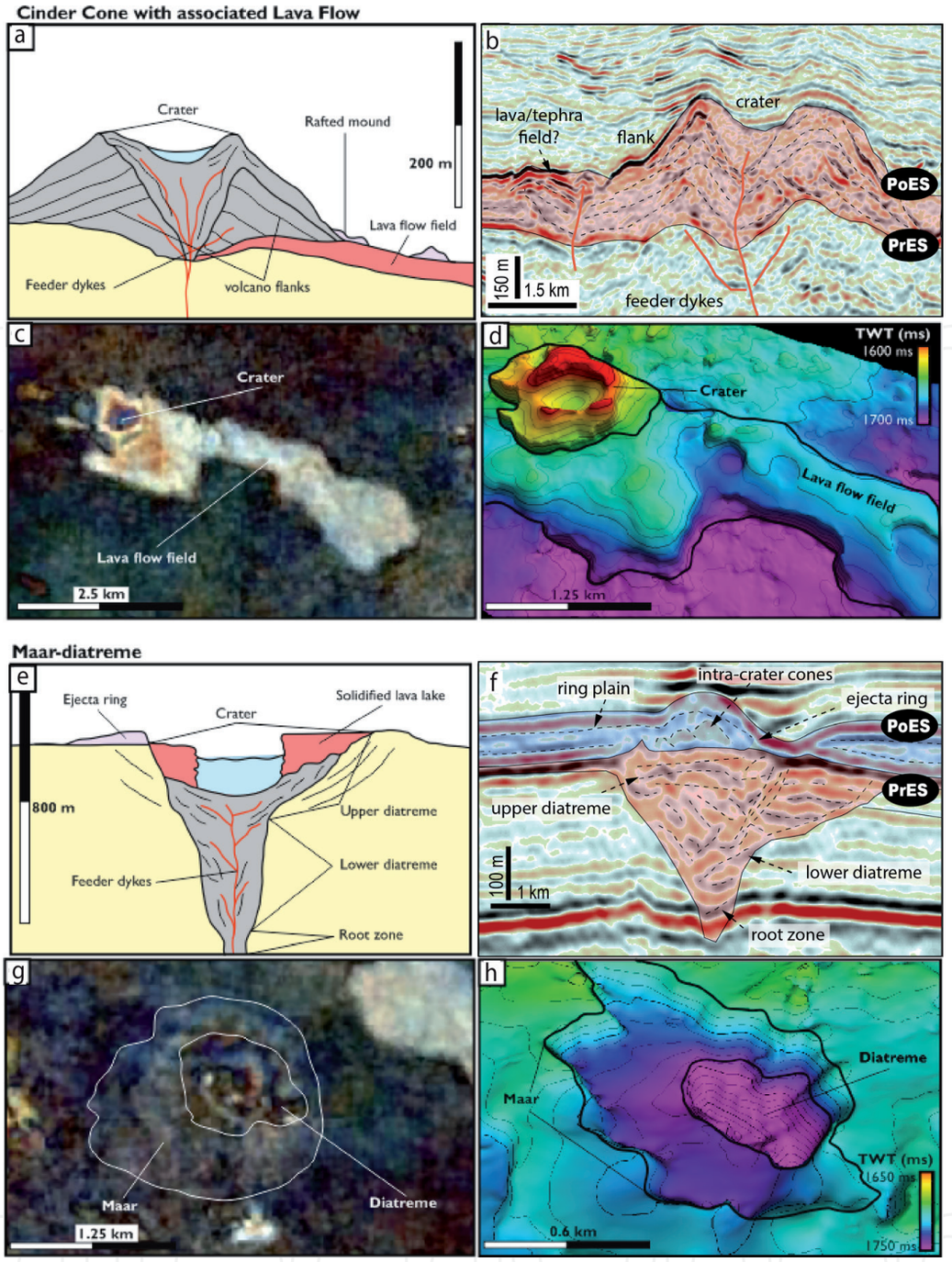

Figure 10.
Illustrations of the architecture of small-volume cones and craters. (a) Schematic cross-section through a cinder cone adapted from Kereszturi and Németh [6]. (b) Seismic cross-section highlighting the general morphology and seismic response of a cinder cone and associated lava field buried offshore Taranaki Basin, New Zealand. Note the characteristic inward-dipping reflections towards the crater and the outward-dipping structure away from the vent zone. (c) Plan view spectral decomposition of the cinder cone taken from the Winnie 3D survey, Eromanga Basin, Australia, highlighting the cone-shaped morphology of the vent and associated extensive lava field [9]. (d) Horizon mapping of the top surface of the cinder cone shown in (c). (d) Cross-section through a maar-diatreme adapted from Kereszturi and Németh [6]. (f) A seismic line across a maar-diatreme volcano buried in the offshore Banks Peninsula, New Zealand [22]. The chaotic reflections indicate deep excavations of the pre-eruptive subsurface. (g) Plan view spectral decomposition of a maar-diatreme buried in the Eromanga Basin, Australia [9]. (h) Oblique, TWT view of the proposed maar-diatreme in (g).

The deduction of mounds- and crater-shaped seismic anomalies being igneous in origin can be reinforced by the presence of artefacts such as pull-up of seismic velocities (**Figure 6a**), indicating that rocks within the anomalies have a much higher acoustic velocity than the surrounding strata [25, 35]. In addition, doming of reflectors overlying mound-shaped volcanoes (**Figure 8a**) is common where

volcanic rocks are less compacted than surrounding sedimentary strata [59, 63]. Seismic interpretation shows that clusters of small craters and cones are often located above the tips of saucer-shaped intrusions or associated with high-amplitude reflections emplaced into pre-eruptive strata (**Figures 6, 8** and **10**), which suggest that magma is likely to stall in numerous interconnected batches immediately below volcanic fields [43, 89]. Multiple craters and cones have been interpreted to form hydrothermal vent complexes where shallow intrusions were emplaced within sedimentary strata [59, 110]. If the magma intrudes into organic-rich sedimentary sequences, these vent complexes could release large amounts of greenhouse gases from metamorphic aureoles, potentially triggering global warming events such as the Paleocene-Eocene Thermal Maximum; PETM [108, 111].

4.3 Large composite, shield and caldera volcanoes

Large (i.e. >5 km^3) composite, shield and caldera volcanoes are discrete landforms constructed over tens to millions of years by repeated eruptions at a relatively confined vent site [7]. The most distinctive large volcanoes are cone-shaped stratovolcanoes, overlapping compound edifices, low-profile shield volcanoes, and ring-shaped caldera depressions. Typically formed by polygenetic building mechanisms, these large volcanoes represent end-member variants with a broad spectrum of intermediary elements. The range of morphologies of polygenetic volcanoes can overlap with each other through time, complicating development of empirical models for interpreting the factors controlling their edifice growth mechanisms and evolution [112]. Each of these large volcanic landforms can be constructed from magmas of any known chemical composition and in all known tectonic settings [72].

Conversely, some particular morphologies are more likely to be developed in specific tectonic conditions and under the influence of certain magmas, allowing us to recognise generalities for each volcanic type. For example, andesitic-dacitic composite volcanoes are commonly derived from partial melting of the asthenosphere at subduction zones, often erupting along volcanic arcs such as the Andes in South America and the Cascades in western USA [5]. The viscosity of andesitic-dacitic magmas favours accumulation of lava and tephra near the eruptive site, building composite morphologies such as stratovolcanoes (e.g. Mt. Fuji, Japan) and compound volcanoes (e.g. Mt. Tongariro, New Zealand). Stratovolcanoes display large (ca 2 km high and 15 km wide) steep-sided (up to 30° slopes) flanks located next to a relatively stationary central vent (**Figure 11**). Whereas, compound volcanoes are formed by several overlapping edifices that together shape a distinctive massif of volcanic rocks separated from other adjacent volcanoes (**Figure 12**). Both strato- and compound volcanoes typically comprise accumulations of interbedded lava-flows, pyroclastic material and reworked volcanic debris [113]. Primary volcanic and epiclastic accumulations follow a proximal-distal facies pattern in which thick, amalgamated and coarser-grained layers are deposited close to the vent zone, while thin, tabular and fine-grained facies accumulate distally to the vent (**Figure 7**). The overall architecture of a composite volcano comprises a central vent zone and overlapping flanks circled by a radial ring-plain deposited around an individual edifice or a group of edifices. In addition, the flanks of composite volcanoes often contain small parasitic cinder cones and lava domes [114].

Shield volcanoes are typical products of low viscosity basaltic lavas erupted at intraplate hotspots, generally associated with extensional settings such as the Hawaiian volcanoes [115]. However, shield volcanoes are also commonly found along intracontinental rifts (e. g. Dama Ali, eastern Ethiopia) and subduction-related volcanic arcs (e.g. Payun Matru, Argentina). Basaltic shield volcanoes consist of a central summit vent (which may or may not include a caldera), enclosed

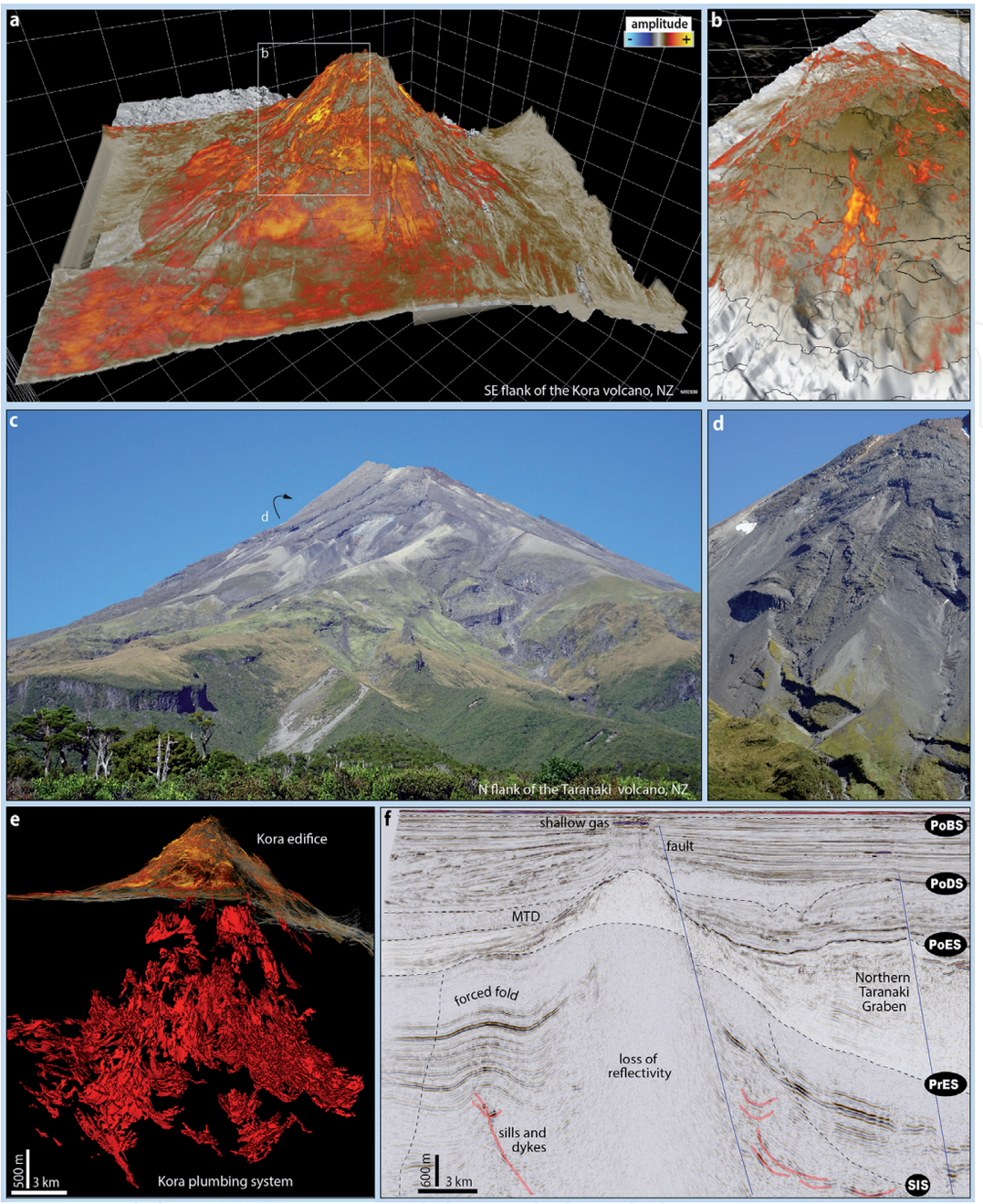

Figure 11.
Seismic and outcrop examples of large (>5 km³) composite volcanos. This type of volcanic landform typically constitutes a single cone-shaped body with a central vent located at or near the summit of the volcano. (a and b) 3D perspective of a rendered amplitude seismic cube across the Kora volcano, New Zealand. (c and d) View of the north flank of the Taranaki volcano, New Zealand. Note the disrupted and channelised geometry of proximal deposits, while distal deposits typically are lobate and more continuous. In (b), the high-amplitude reflections (red) are discontinuous and disrupted, which likely reflect multiple depositional and erosional events, such as observed to form at the flanks of Taranaki volcano (d). (e) Oblique 3D view of the intrusive and extrusive parts of the Kora volcano. The edifice is highlighted by an opacity rendered amplitude cube, while the plumbing system was mapped as numerous interconnected geobodies. (f) Amplitude display of a seismic section across the Kora volcano.

by low-angle (<10° slopes) peripheral flanks, and a flat lava apron that can extend tens of km's from the vent [116]. Parasitic vents commonly erupt on the flanks of shield volcanoes, often forming rows of spatter and scoria cones aligned with normal faults (**Figure 13**). In addition, oceanic and paralic shield volcanoes are likely to contain a hyaloclastite apron and associated lava-deltas, in which interaction between lava and seawater may trigger hydrovolcanic explosions that can produce large amounts of fragmented material [117].

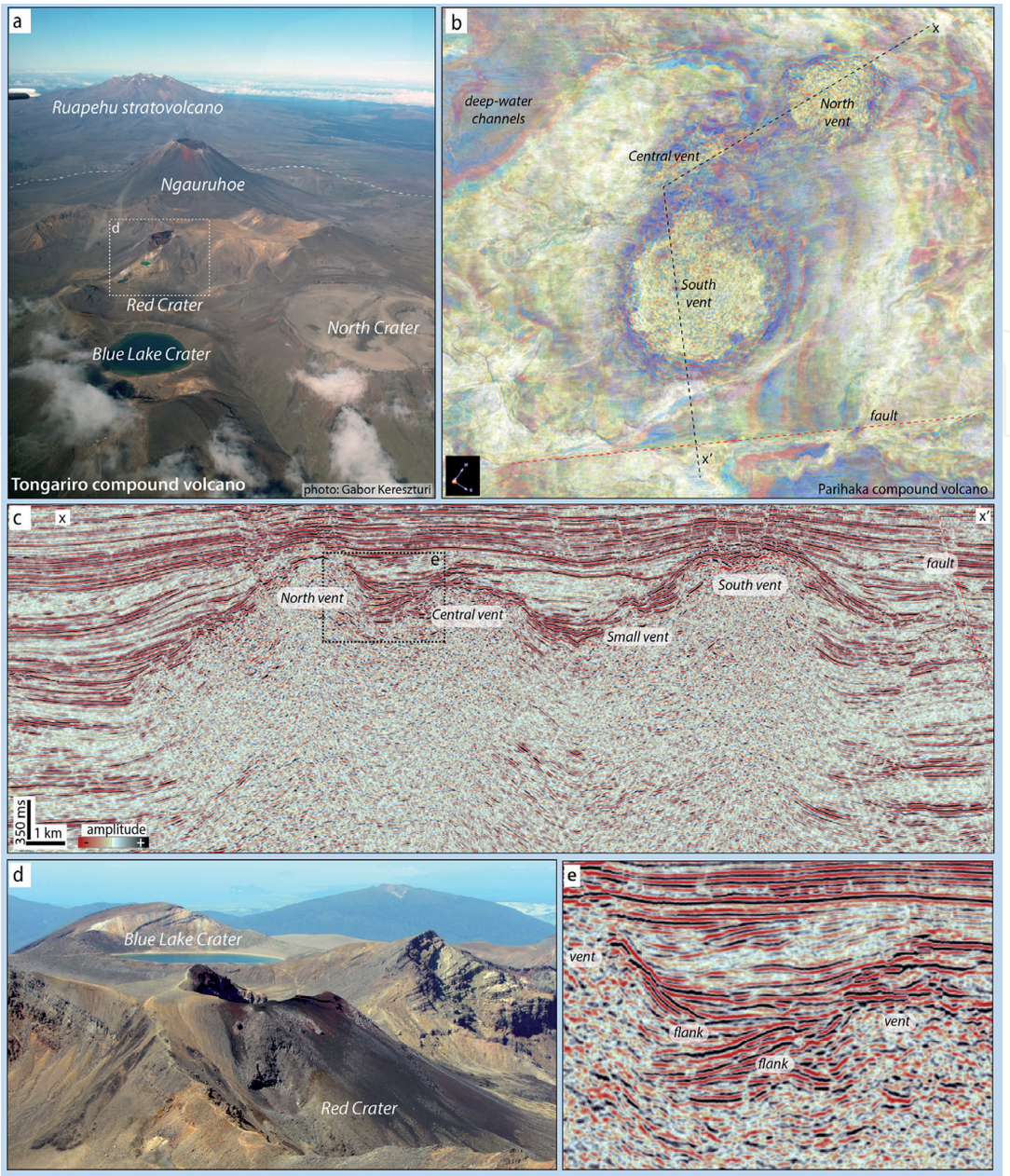

Figure 12.
Seismic and outcrop examples of large (>5 km³) compound volcanoes. Several overlapping vents which are typically randomly distributed characterise this type of volcanic landform. (a) An aerial view of the southern sector of the Tongariro compound volcano with the Ruapehu stratovolcano in the background. (b) Plain view over a rendered amplitude seismic cube showing the location of three main vents within the Parihaka compound volcano, New Zealand. (c) Amplitude display of a seismic section across the Parihaka volcanoes. Note the overlapping flanks of the main vents. (d) Photograph from the summit of the Ngauruhoe volcano showing a detailed view of the Red Crater, Blue Lake Crater and overlapping lavas of the Mangahouhounui Fm, Tongariro compound volcano. (e) Detail of the amplitude display of a seismic section shown in (c). Note the overlapping reflections on the flanks of the vents.

Large polygenetic volcanoes have been interpreted from seismic reflection datasets since the 1980s' in many sedimentary basins globally. Similar to their smaller cone and crater equivalents (Section 4.2), the reflection configuration within and around large buried volcanoes may make it possible to interpret their broad architecture and genesis. Buried composite and shield volcanoes typically resemble small mound- and cone-shaped vents (**Figures 10–13**). Therefore, their architecture comprises chaotic and inward-dipping reflections at the vent zone, continuous to discontinuous reflections at the flanks, and a wide, almost flat ring plain evident by high-to-moderated amplitude reflections that pinch and fade with increasing

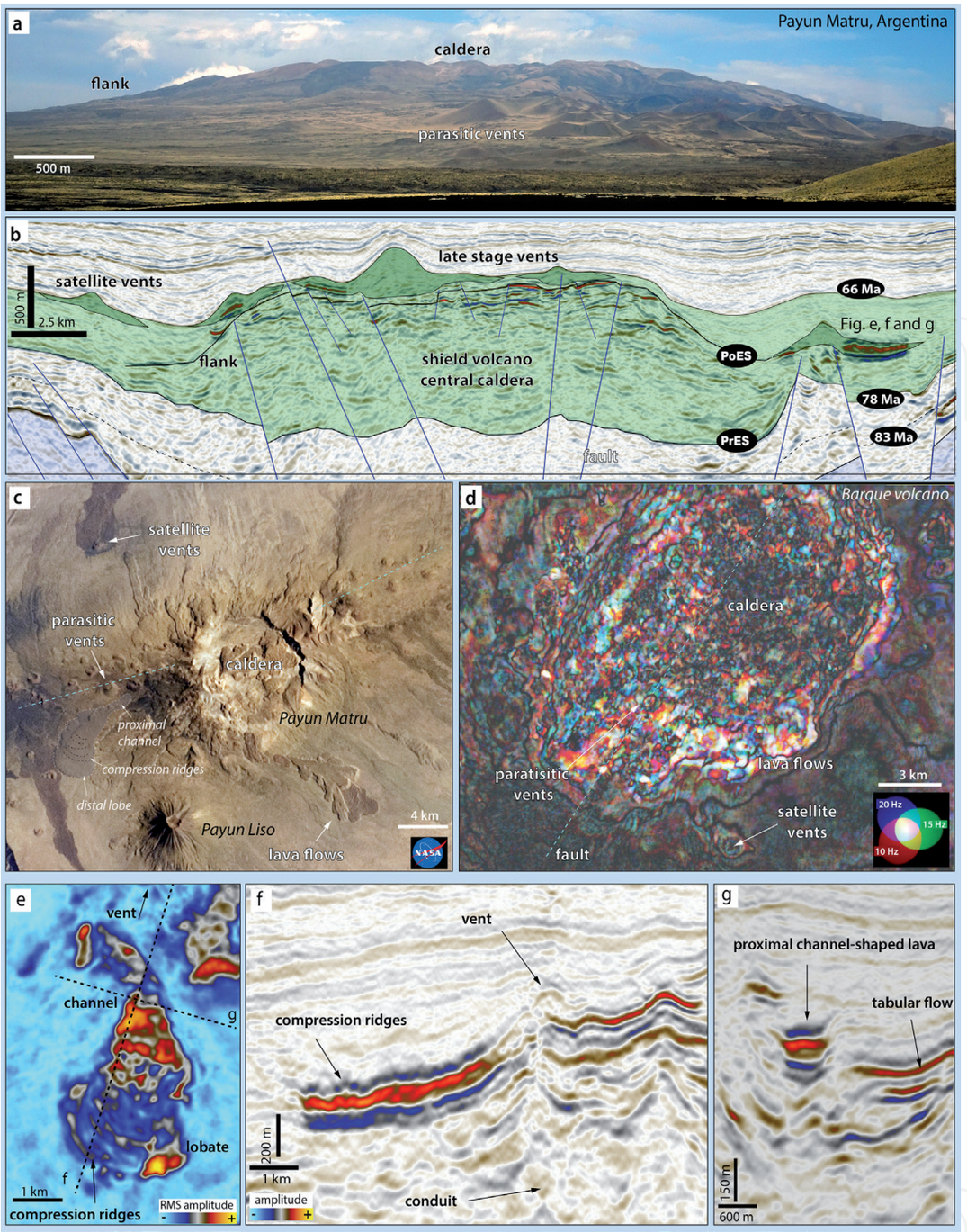

Figure 13.
Seismic and outcrop examples of shield volcanoes with a central caldera. (a) Photograph of the northern flank of the Payun Matru Volcano, Argentina. (b) Amplitude display of a seismic section across the Barque volcano, offshore Canterbury Basin, New Zealand (Modified from [28]). (c) Aerial view of the region of the Payun Matru, a shield with a central caldera, and Payun Liso a stratovolcano. Note the NW alignment of cinder cones. (d) Plain view of a decomposed seismic cube showing the flanks and central depression of the Barque volcano. Parasitic and satellite vents are commonly aligned with normal faults. (e) Plain view of an RMS seismic cube across a lava flow of the Barque volcano. (f and g) Amplitude display of a seismic section across the lava flow in (e).

distance from the main volcanic body [1, 63]. Parasitic and satellite vents are often described on the flanks of these large buried volcanoes, typically located above pre-existing structures of the basement or at radial normal faults [52]. Interpretation of seismic reflection datasets suggests that the shallow (<5 km) plumbing system of large polygenetic volcanoes comprises a myriad of interconnected intrusive bodies, mainly aligned with crustal structures, markedly contrasting with the classic "balloon-and-straw" model [24, 28, 118].

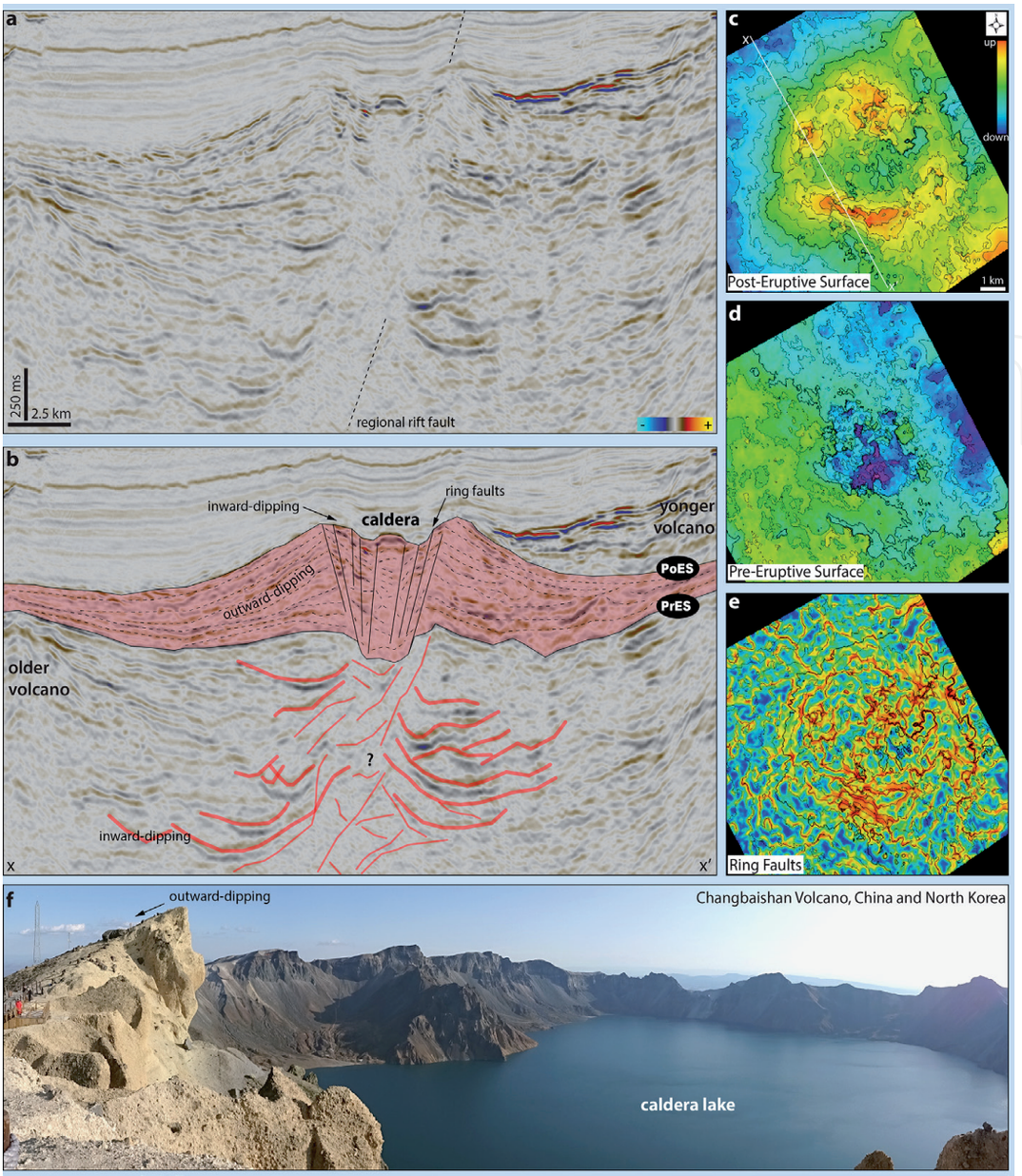

Figure 14.
Seismic and outcrop examples of shield volcanoes with a central caldera. (a) Uninterpreted and (b) interpreted amplitude display of a seismic section across the Hades caldera, offshore Deepwater Taranaki Basin, New Zealand (Modified from [28]). (c) Post-eruptive surface and (d) pre-eruptive surface isochron horizon maps of the Hades caldera. Note the wide (ca 5 km) central depression with inward-dipping reflections circled by a ring of outward-dipping layered material. (e) Pre-eruptive surface isochron horizon map applying an edge-detection attribute, which is enhancing a series of ring-shaped faults at the location of the caldera depression. (f) Photograph of the crater lake at the summit of the Changbaishan Volcano, Chinese and North Korean border. The lake marks the location of a 5 km wide caldera vent formed by a large pyroclastic eruption in 946 AD. Note the steeply inclined outward-dipping layers of white ignimbrite rocks at the left corner of the picture.

Caldera-forming volcanoes are commonly associated with subsidence and collapse of the roof of magma chambers due to partial withdrawal of magma during voluminous and short-lived eruptions [119]. Characteristic caldera volcanoes are silicic in composition and produced by ultra-Plinian eruptions, often developing in association with rifted arcs such as the Taupo Volcanic Zone in New Zealand [120, 121]. However, smaller pyroclastic and non-explosive calderas of more mafic compositions often form within the central vent zone of composite and shield volcanoes [122]. Caldera volcanoes have a variety of geometries and structures mainly defined by mechanisms of pyroclastic material dispersal, caldera collapse,

and dome resurgence [123]. The general architecture of large silicic calderas comprises a central depression of 1–2 km depth surrounded by lateral by an ignimbrite plateau or steepen flanks of pyroclastic and lava material, which can cover areas of >3000 km^2 [72]. The central depression is often bounded by ring faults and hosts thick sequences of intra-caldera pyroclastic deposits, late-stage andesitic-rhyolitic lava-flows and domes, lacustrine sediments and debris. Caldera volcanoes may or may not produce a post-eruptive resurgent dome, a consequence of intra-caldera uplift from a renewed rise of magma into the chamber(s), such as documented from the Toba Volcano, Indonesia, and Yellowstone, USA [124].

Interpretation of buried caldera volcanoes from seismic data is scarce, and to our knowledge, only documented in two places offshore New Zealand [28]. Barque volcano, offshore Canterbury Basin, is potentially a large (ca 20 km wide) shield volcano with a central caldera (**Figure 13**). Hades caldera, in the Deepwater Taranaki, has a semi-circular structure 10 km across with a central depression 3.5 km wide and 1 km deep bounded by ring faults, likely formed by pyroclastic mechanisms of material fragmentation and dispersion (**Figure 14**). Both examples show no evidence of a single large batch of magma sited beneath the caldera. Rather, multiple interconnected intrusions, including saucer-shaped sills and tabular bodies aligned with pre-and syn-rift faults more likely describe their magma plumbing systems (**Figures 13** and **14**).

4.4 Voluminous lava fields

Eruptions of voluminous (i.e. >10,000 km^3) lava fields are commonly associated with continental break-up and upwelling of mantle plumes that form Large Igneous Provinces (LIPs). Characteristically, LIPs comprise extensive flood basalt plateaus derived from decompression melting of the mantle, but more differentiated alkalic, tholeiitic, and silicic rocks can also occur as lavas, pyroclastic, and intrusive bodies [125]. LIPs constitute the most extensive volcanic landscapes on Earth, including regional-scale igneous-dominated structures such as continental flood basalts, volcanic rifted margins, oceanic plateaus, submarine ridges, seamount chains, and ocean-basin flood basalts [126]. The voluminous lava fields often erupt at both continental (e.g. Siberian Traps, Asia) and oceanic crust (e.g. Ontong Java Plateau, Pacific Ocean), as well as at divergent plate boundaries such as the South Atlantic Margins [127].

The broad architecture of LIPs consists of stacks of sub-horizontal sheets of lava flows up to ca 10 km thick underlying by networks of subvolcanic sills and dykes [51, 128]. The extrusive part of LIPs is interpreted to be mainly fed by repeated voluminous eruptions sourced from scattered fissure vents and shield volcanoes, in which the entire volcanic pile is typically constructed in relatively short time spans (<1 Myr). Individual flows can reach volumes as much as 1000 km^3 and extend for hundreds of kilometres from the vent site, such as described in the Columbia River Plateau and the Deccan Traps [72]. The Laki eruption in Iceland, for example, is one of the largest documented historical lava flows. It covered an area of near 600 km^2 of southern Iceland in the 1780s, with an estimated discharge of almost 15 km^3 of lava from a 27 km long fissure vent system consisting of scoria, spatter, and tuff cones [129].

Most voluminous lava fields are interbedded with sedimentary basins formed by crustal extension, rifting, and continental drifting [130]. Volcanic rift margins have been the most intensively studied LIPs from seismic reflection datasets (**Figure 15**). Over the past 40 years, interpretation of enormous amounts of seismic data along the boundaries of the Atlantic, Western Australian, and Southern Indian continental crusts showed that rift margins typically comprise a set of characteristic volcanic seismic facies units [4, 11, 131]. These seismic facies units represent interactions between

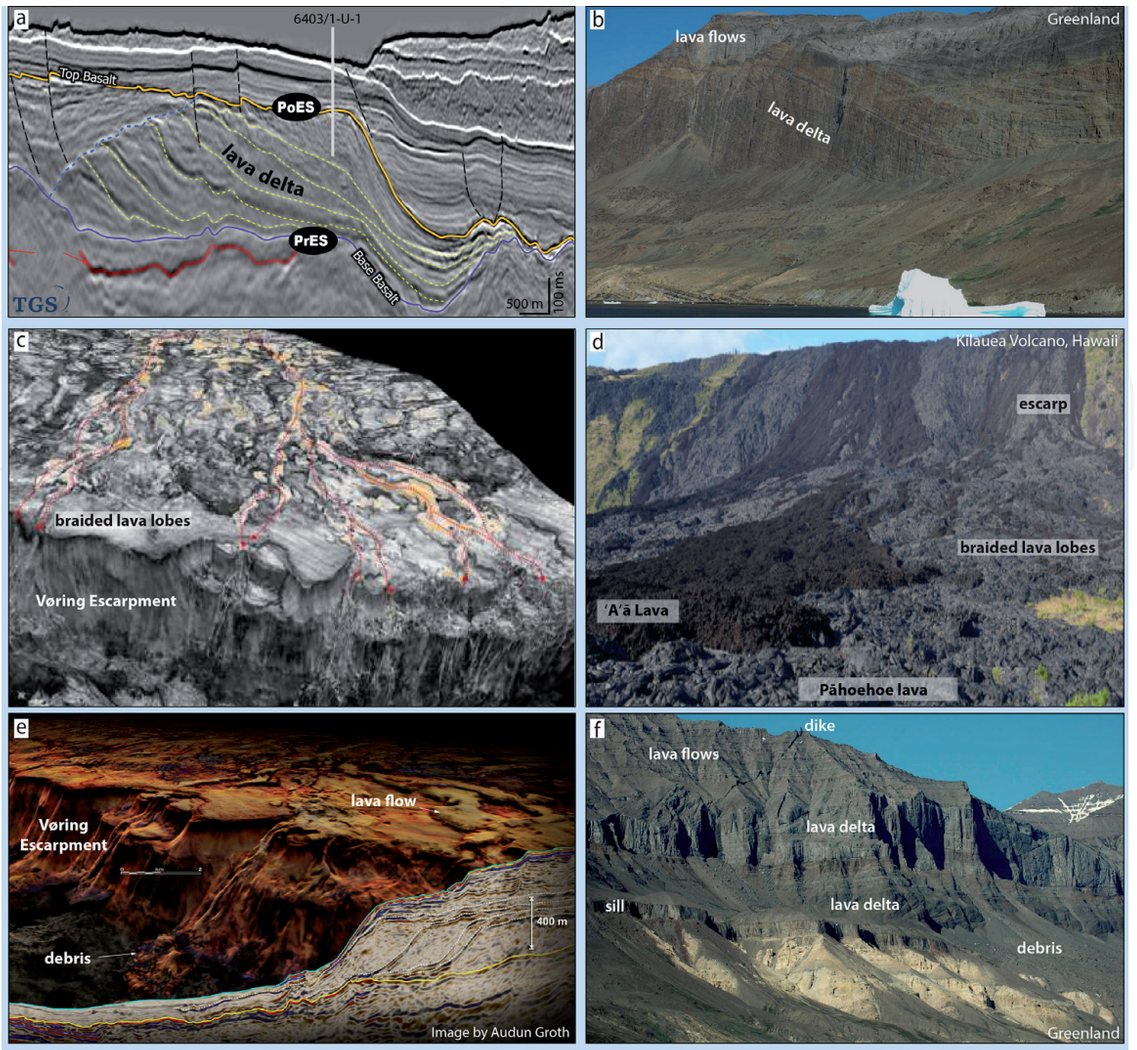

Figure 15.
Seismic and outcrop examples of volcanic rift margins and lava-fields. (a) Amplitude display of a seismic section across the Kolga Lava Delta, offshore Norway, showing the characteristic wedge of progradational deltas (From [45]). (b) Prograding foresets of a lava delta in western Greenland. (c) Perspective view of the top-basalt horizon of the Vøring Escarpment, offshore Norway (From [29]). (d) Lava field and escarpments formed during the 2018 series of eruptions of the Kilauea Volcano, Hawaii. (e) Perspective view of the Vøring Escarpment (From [29]). (f) Geometric relationship of intrusive and extrusive bodies of a voluminous lava field in western Greenland. Data courtesy of TGS (a).

volcanism and sedimentation, and their interpretation informs the construction of models for the initiation and evolution of volcanic rift margins [26]. The typical volcanic rift margin sequence initiates with aggradation of peperites, hydrobreccias, and pillow-lavas where magma interacts with water and wet sediments, while subaerial lava-flows can develop at the basin margins and on topographic highs [132]. Continued aggradation and progradation of igneous material favours more effusive and subaerial volcanism, in which eruptions tend to form extensive sheets of stacked lava-flow deposits [34]. If the lava-flows stretch an existing shoreline, a prograding lava-delta comprising of hyaloclastic and epiclastic material can be developed [133]. Subsequently, these volcanic deposits may be exposed to erosional conditions, forming escarpments surfaces, slumps, and volcaniclastic gravity flow deposits triggered by degradation of the volcanic sequence [134].

A recent seismic geomorphological study used a 2500 km^2 high-quality 3D seismic survey to image the top-basalt horizon of the Vøring Marginal High, offshore Norway [29]. Interpretation of this seismic horizon revealed a series of volcanic macroforms such as lava-flows with compressional ridges and braided lava-channels

with similar structure and size of morphologies described in modern subaerial lava fields (**Figure 15**). In addition, the Vøring Marginal High 3D data showed numerous pitted and irregular lava surfaces next to smooth sheet-like reflections with geometry comparable to fields of small cone and crater volcanoes and their associated peripheral lava flows. These pitted seismic features are interpreted to correspond to places where magma was emplaced into wet sediments or water [29]. Debris flows deposits along with large slumped blocks are well imaged at the top of the Vøring Escarpment, revealing a volcanic morphology influenced by erosion and degradation of pre-existing voluminous lava fields (**Figure 15**).

5. Conclusions

Interpretation of 2D and 3D seismic reflection datasets provides valuable insights into the morphology and stratigraphic signature of entire igneous systems buried in sedimentary basins. The application of 3D seismic visualisation methods offers a unique opportunity for direct comparison of the geomorphic aspects of buried and outcropping volcanoes, with resolutions down to tens of metres.

Buried volcanic systems comprise a network of intrusive, eruptive, and sedimentary architectural elements with length scales of 10^2–10^4 meters that are recognisable from both seismic and outcrop analyses. These architectural elements often show a spatial and temporal distribution controlled by their distance from eruptive centres. The geometry and internal arrangement of facies within these elements reflect a range of physical factors including, magma composition, effusion discharge rate, degree of material fragmentation, and the presence or absence of water at the eruption vent. Many, if not most, volcanic systems are underlain by shallow (<5 km) interconnected networks of sills, saucer-sills, laccoliths, dykes, and hybrid intrusions that often align with pre-existing crustal structures or contemporaneous faults.

Description and interpretation of seismic reflection surveys together with their outcropping volcano analogues from key localities worldwide suggest three main geomorphic categories of buried volcanoes. These categories are (1) clusters of small-volume (<1 km^3) craters and cones, including maar-diatremes, tuff rings, spatter cones, scoria cones, tuff cones, and hydrothermal vent complexes, (2) large (>5 km^3) composite, shield and caldera volcanoes, and (3) voluminous lava fields (>10,000 km^3). This classification of buried volcanoes is based on their geometry, size, and spatio-temporal distribution of eruptive centres, and is independent of parameters such as magma composition, tectonic setting, or environment where the eruption occurred. Classifying the buried volcanoes into geomorphic categories helps us to understand the processes that link their endogenous and exogenous realms, providing insights into the architecture, edifice growth mechanisms and longevity of igneous systems buried in sedimentary basins.

The modern methods of seismic interpretation, from 2D regional scale to detailed 3D analysis, can provide an accurate understanding of the geological processes that formed the volcanoes now buried in the subsurface. Realistic models for the facies distribution and architecture of buried volcanoes can be constrained by their geomorphic similarities to outcropping volcanoes, establishing the principles for the new discipline of seismic-reflection volcanology.

Acknowledgements

We would like to thank the Ministry of Business, Innovation and Employment (MBIE) of New Zealand and TGS for access to seismic and well data, and IHS

Markit and Schlumberger for providing academic licence to use Kingdom and Petrel software. AB thanks funding from the MBIE research grant UOCX1707. SP acknowledges support from the Norwegian Research Council Centres of Excellence funding scheme (CEED; project number 223272). We appreciate the constructive reviews of Ray Cas and Jim Cole, and the contribution of Jessica Fensom in proof-reading and discussing the manuscript.

Conflict of interest

The authors declare no conflict of interest.

Author details

Alan Bischoff[1*], Sverre Planke[2], Simon Holford[3] and Andrew Nicol[1]

1 University of Canterbury, Christchurch, New Zealand

2 VPBR and University of Oslo, Oslo, Norway

3 University of Adelaide, Adelaide, Australia

*Address all correspondence to: alan.bischoff@canterbury.ac.nz

References

[1] Herzer RH. 1995. Seismic Stratigraphy of a Buried Volcanic Arc, Northland, New Zealand and Implications for Neogene Subduction. Marine and Petroleum Geology 12, no. 5 511-31. https://doi.org/10.1016/0264-8172(95)91506-K.

[2] Magee C, Hunt-Stewart E, Jackson CAL. 2013. Volcano growth mechanisms and the role of sub-volcanic intrusions: Insights from 2D seismic reflection data: Earth and Planetary Science Letters, doi:10.1016/j.epsl.2013.04.041.

[3] Planke S, Alvestad E, Eldholm O. 1999. Seismic Characteristics of Basaltic Extrusive and Intrusive Rocks. The Leading Edge 18 (3): 342. doi:10.1190/1.1438289.

[4] Planke S, Symonds PA, Alvestad E, Skogseid J. 2000. Seismic Volcanostratigraphy of Large-Volume Basaltic Extrusive Complexes on Rifted Margins. J Geophys Res 105 (B8): 19335. https://doi.org/10.1029/1999JB900005

[5] Grosse P, van Wyk de Vries B, Petrinovic IA, Euillades PA, Alvarado GE. 2009. Morphometry and evolution of arc volcanoes. Geology 37 (7), 651e654. http://dx.doi.org/10.1130/G25734A.1.

[6] Kereszturi G, Németh C. 2012. Monogenetic Basaltic Volcanoes: Genetic Classification, Growth, Geomorphology and Degradation: Updates in Volcanology - New Advances in Understanding Volcanic Systems, https://doi.org/10.5772/51387

[7] Manville V, Nemeth K, Kano K. 2009. Source to sink: A review of three decades of progress in the understanding of volcaniclastic processes, deposits, and hazards. Sedimentary Geology. 136-161. 10.1016/j.sedgeo.2009.04.022.

[8] Planke et al. 2018. Seismic Imaging and Petroleum Implication of Igneous Intrusions in Sedimentary Basins.

[9] Hardman JPA, Holford SP, Schofield N, Bunch M, Gibbins D. 2019. The Warnie volcanic province: Jurassic intraplate volcanism in Central Australia. Gondwana Research 76, 322-347. https://doi.org/10.1016/j.gr.2019.06.012

[10] Berndt C, Planke S, Alvestad E, Tsikalas F, Rasmussen T. 2001. Seismic volcanostratigraphy of the Norwegian Margin: Constraints on tectonomagmatic break-up processes: Journal of the Geological Society, 158, 413-426, doi: 10.1144/jgs.158.3.413.

[11] Calvès G, Schwab AM, Huuse M, Clift PD, Gaina C, Jolley D, Tabrez AR, Inam A. 2011. Seismic volcano-stratigraphy of the western Indian rifted margin: The pre-Deccan igneous province, J. Geophys. Res., 116, B01101, doi:10.1029/2010JB000862.

[12] Carlotto MA, Silva RCB, Yamato AA, Trindade WL, Moreira JLP, Fernandes RAR, Ribeiro OJS, et al. 2017. Libra: A Newborn Giant in the Brazilian Presalt Province. In Giant Fields of the Decade 2000-2010. doi:10.1306/13572006M1133685.

[13] Field BD, Browne GH, Davy BW, Herzer RH, Hoskins RH, Raine JI, Wilson GJ, Sewell RJ, Smale D, Watters WA. 1989. Cretaceous and Cenozoic sedimentary basins and geological evolution of the Canterbury region, South Island, New Zealand. Lower Hutt: New Zealand Geological Survey. New Zealand Geological Survey Basin Studies 2: 94.

[14] Paumard V, Zuckmeyer E, Boichard R, Jorry S, Bourget J, Borgomano J, Maurin T, Ferry JN, 2017, Evolution of Late Oligocene - Early Miocene attached and isolated

carbonate platforms in a volcanic ridge context (Maldives type), Yadana field, offshore Myanmar: 361-387 p., doi:10.1016/j.marpetgeo.2016.12.012.

[15] Reynolds P, Holford S, Schofield N, Ross A. 2017. Three-Dimensional Seismic Imaging of Ancient Submarine Lava Flows: An Example From the Southern Australian Margin. Geochem. Geophys. Geosys. doi:10.1002/2017GC007178

[16] Sacchi et al. 2019. The use and beauty of ultra-high-resolution seismic reflection imaging in Late Quaternary marine volcaniclastic settings, Napoli Bay, Italy. Földtani Közlöny. 149. 371. DOI: https://doi.org/10.23928/foldt.kozl.2019.149.4.371

[17] Sun QL, Wu SG, Cartwright J, Wang SH, Lu YT, Chen DX, Dong DD. 2014. Neogene igneous intrusions in the northern South China Sea: Evidence from high resolution three dimensional seismic data. Marine and Petroleum Geology, 54, 83– 95. https://doi.org/10.1016/j.marpetgeo.2014.02.014

[18] Davies RJ, Posamentier HW, Wood LJ, Cartwright J. 2007. Seismic Geomorphology: Applications to Hydrocarbon Exploration and Production. Geological Society Special Publications. DOI: https://doi.org/10.1144/GSL.SP.2007.277.01.01

[19] Hart BS. 2013. Whither seismic stratigraphy? Interpretation 1(1): SA3–SA20. https://doi.org/10.1190/INT-2013-0049.1

[20] Posamentier HW, Kolla V. 2003. Seismic Geomorphology and Stratigraphy of Depositional Elements in Deep-Water Settings. J. Sed. Res., 73 (3), 367-88., doi:10.1306/111302730367

[21] Cas RAF, Wright JV. 1987. Volcanic Successions: Modern and Ancient - A Geological Approach to Processes, Products and Successions. Chapman and Hall, UK, https://doi.org:10.1007/978-0-412-44640-5

[22] Bischoff AP, Rossetti M, Nicol A, Kennedy B. 2019b. Seismic Reflection and Petrographic Interpretation of a Buried Monogenetic Volcanic Field (Part 1). Bull Volcanol 81: 56. https://doi.org/10.1007/s00445-019-1316-7

[23] McLean CE, Schofield N, Brown DJ, Jolley DW, Reid A. 2017. 3D seismic imaging of the shallow plumbing system beneath the Ben Nevis Monogenetic Volcanic Field: Faroe–Shetland Basin: J. Geol. Soc. https://doi.org/10.1144/jgs2016-118

[24] Walker F, Schofield N, Millett J, Jolley D, Holford S, Planke S, Jerram DA, Myklebust R. 2020. Inside the volcano: Three-dimensional magmatic architecture of a buried shield volcano. Geology doi: https://doi.org/10.1130/G47941.1

[25] Holford SP, Schofield N, MacDonald JD, Duddy IR, Green PF. 2012, Seismic Analysis of Igneous Systems in Sedimentary Basins and Their Impacts on Hydrocarbon Prospectivity: Examples from the Southern Australian Margin. APPEA Journal, 52, 229-52.

[26] Planke S, Svensen H, Myklebust R, Bannister S, Manton B, Lorenz L. 2015. Geophysics and remote sensing, Advances in Volcanology: Springer, 1-16.

[27] Reynolds P, Schofield N, Brown RJ, Holford SP. 2016. The architecture of submarine monogenetic volcanoes - insights from 3D seismic data: Basin Research, v. 30, p. 437-451, doi:10.1111/bre.12230.

[28] Bischoff A, Barrier A, Beggs M, Nicol A, Cole J. 2020. Volcanoes Buried in Te Riu-a-Māui/Zealandia Sedimentary Basins. In: IAVCEI Special Issue: Cenozoic Volcanism in New Zealand. New Zealand Journal of

Geology and Geophysics. 63:4, 378-401. https://doi.org/10.1080/00288306.2020.1773510

[29] Planke S, Millett JM, Maharjan D, et al. 2017. Igneous seismic geomorphology of buried lava fields and coastal escarpments on the Vøring volcanic rifted margin: Interpretation, doi:10.1190/INT-2016-0164.1.

[30] Marfurt K. 2018. Seismic Attributes as the Framework for Data Integration Throughout the Oilfield Life Cycle: Society of Exploration Geophysicists, 508 p., doi: doi:10.1190/1.9781560803522.

[31] Sheriff RE, Geldart LP. 1995. Exploration Seismology, 2nd edn., Cambridge University Press, Cambridge, UK.

[32] Vail PR, Mitchum RM, Todd RG, Widmier JM, Thompson S, Sangree JB, Bubb JN, Hatlelid WG. 1977. Seismic stratigraphy and global changes of sea-level. In: Payton, C.E. (Ed.), Seismic Stratigraphy – Applications to Hydrocarbon Exploration. AAPG Memoir 26, pp. 49-212

[33] Heap MJ, Kennedy BM. 2016. Exploring the scale-dependent permeability of fractured andesite: Earth and Planetary Science Letters, doi:10.1016/j.epsl.2016.05.004.

[34] Millett J, Hole M, Jolley D, Schofield N, Campbell E. 2015. Frontier exploration and the North Atlantic Igneous Province: New insights from a 2.6 km offshore volcanic sequence in the NE Faroe–Shetland Basin. Journal of the Geological Society. 173. 10.1144/0016-76492015-069.

[35] Jackson CAL. 2012. Seismic reflection imaging and controls on the preservation of ancient sill-fed magmatic vents. J. Geol. Soc. https://doi.org/10.1144/0016-76492011-147

[36] Rateau R, Schofield N, Smith M. 2013. The potential role of igneous intrusions on hydrocarbon migration, West of Shetland: Petroleum Geoscience, 19, 259-272, doi:10.1144/petgeo2012-035.

[37] Bischoff AP, Nicol A, Barrier A, Wang H. 2019a. Paleogeography and Volcanic Morphology Reconstruction of a Buried Monogenetic Volcanic Field (Part 2). Bull Volcanol 81: 57. https://doi.org/10.1007/s00445-019-1317-6

[38] Klarner S, Klarner O. 2012. Identification of Paleo-Volcanic Rocks on Seismic Data. In: Updates in Volcanology-A Comprehensive Approach to Volcanological Problems, IntechOpen, 181-206 pp.

[39] Rohrman M. 2007. Prospectivity of Volcanic Basins: Trap Delineation and Acreage de-Risking. AAPG Bulletin. 91 (6), 915-39., doi:10.1306/12150606017

[40] Mordensky S, Villeneuve M, Farquharson J, Kennedy B, Heap MJ, Gravley DM. 2018. Rock mass properties and edifice strength data from Pinnacle Ridge, Mt. Ruapehu, New Zealand: doi:10.1016/j.jvolgeores.2018.09.012.

[41] Schofield N, Jerram DA, Holford S, Stuart A, Niall M, Hartley A, Howell J, David M, Green P, Hutton D, Stevenson C. 2016. Sills in sedimentary basin and petroleum systems: In Németh K (ed) The Series Advances in Volcanology, pp 1-22.

[42] Jerram DA, Single RT, Hobbs RW, Nelson CE. 2009. Understanding the offshore flood basalt sequence using onshore volcanic facies analogues: An example from the Faroe-Shetland basin. Geol. Mag. https://doi.org/10.1017/S0016756809005974

[43] MageeC,StevensonCTE,EbmeierSK, Keir D, Hammond JOS, Gottsmann JH, Whaler KA, Schofield N, Jackson CAL, et al. 2018. Magma Plumbing Systems:

A Geophysical Perspective. Journal of Petrology, egy064, https://doi.org/10.1093/petrology/egy064

[44] Infante-Paez L, Marfurt KJ. 2017. Seismic expression and geomorphology of igneous bodies: A Taranaki Basin, New Zealand, case study. Interpretation. 5 (3), SK121-SK140., https://doi.org/10.1190/INT-2016-0244.1

[45] Millett J, Manton BM, Zastrozhnov D, Planke S, Maharjan D, Bellwald B, Gernigon L, et al. 2020. Basin structure and prospectivity of the NE Atlantic volcanic rifted margin: cross-border examples from the Faroe–Shetland, Møre and Southern Vøring basins. Geological Society, London, Special Publications, 495, 7 January 2020, https://doi.org/10.1144/SP495-2019-12

[46] Catuneanu O, Abreu V, Bhattacharya JP, Blum MD, Dalrymple RW, Eriksson PG, Fielding CR, Fisher WL, Galloway WE, Gibling MR, et al. 2009. Towards the standardisation of sequence stratigraphy. Earth-Science Reviews 92, 1-33. Elsevier B.V.: 1-33. doi:10.1016/j.earscirev.2008.10.003.

[47] Miall AD. 2016. Stratigraphy: A Modern Synthesis: Cham, Springer International Publishing, doi:10.1007/978-3-319-24304-7.

[48] Vail PR, Mitchum RM. 1977. Seismic stratigraphy and global changes of sea level. I: Overview: Memoir American Association of Petroleum Geologists, 22, 51-52.

[49] Abdelmalak MM, Planke S, Faleide JI, Jerram DA, ZastrozhnovD, Eide S, Myklebust R. 2016. The development of volcanic sequences at rifted margins: New insights from the structure and morphology of the Vøring Escarpment, mid-Norwegian Margin: Journal of Geophysical Research, Solid Earth, 121, 5212-5236, doi: 10.1002/2015JB012788.

[50] Jerram DA. 2015. Hot rocks and oil: Are volcanic margins the new frontier? Elsevier R&D Solutions for Oil and Gas, Exploration & Production, https://www.elsevier.com/__data/assets/pdf_file/0008/84887/ELS_Geofacets-Volcanic-Article_Digital_r5.pdf

[51] Svensen H, Torsvik TH, Callegaro S, Augland L, Heimdal TH, Jerram DA, Planke S, Pereira E. 2017. Gondwana Large Igneous Provinces: plate reconstructions, volcanic basins and sill volumes. Geological Society, London, Special Publications. doi:10.1144/SP463.7

[52] Bischoff AP, Nicol A, Beggs M. 2017. Stratigraphy of architectural elements in a buried volcanic system and implications for hydrocarbon exploration: Interpretation. https://doi.org/10.1190/INT-2016-0201.1

[53] Bischoff A, Nicol A, Cole J, Gravely D. 2019c. Stratigraphy of Architectural Elements of a Buried Monogenetic Volcanic System. Open Geosciences, 11(1), pp. 581-616. Retrieved 23 Mar. 2020, from doi:10.1515/geo-2019-0048

[54] Bishop MA. 2009. A generic classification for the morphological and spatial complexity of volcanic (and other) landforms. Geo-morphology 111 (1e2), 104e109.

[55] Cas RAF, Giordano G. 2014. Submarine volcanism: A review of the constraints, processes and products, and relevance to the Cabo de Gata volcanic succession. https://doi.org:10.3301/IJG.2014.46

[56] Cas RAF, Simmons JM. 2018. Why Deep-Water Eruptions Are So Different From Subaerial Eruptions. Front. Earth Sci. 6:198. doi: 10.3389/feart.2018.00198

[57] Németh K. Palmer J. 2019. Geological mapping of volcanic terrains: Discussion on concepts, facies models, scales, and resolutions from

New Zealand perspective. Journal of Volcanology and Geothermal Research, https://doi.org/10.1016/j.jvolgeores.2018.11.028

[58] Barrier A, Bischoff AP, Nicol A, Browne GH, Bassett K. 2020. Identification and morphology of buried volcanoes from the Canterbury Basin, New Zealand. Marine Geology. In review. (In press)

[59] Planke S, Rasmussen T, Rey SS, Myklebust R. 2005. Seismic characteristics and distribution of volcanic intrusions and hydrothermal vent complexes in the Vøring and Møre basins, in Petroleum Geology: North-West Europe and Global Perspectives – Proceedings of the 6th Petroleum Geology Conference. doi:10.1144/0060833.

[60] Bischoff AP. 2019. Architectural Elements of Buried Volcanic Systems and Their Impact on Geoenergy Resources. Ph.D. Thesis, Canterbury University, New Zealand. https://ir.canterbury.ac.nz/handle/10092/16730

[61] Tipper JC. 1993. Do seismic reflections necessarily have chronostratigraphic significance? Geological Magazine, doi:10.1017/S0016756800023712.

[62] Uruski C. 2019. Seismic recognition of igneous rocks of the Deepwater Taranaki Basin, New Zealand, and their distribution. New Zealand Journal of Geology and Geophysics 1-20.

[63] Gatliff RW, Hitchen K, Ritchie JD, Smythe DK. 1984. Internal structure of the Erlend Tertiary volcanic complex, north of Shetland, revealed by seismic reflection: Journal of the Geological Society, v. 141, p. 555-562, https://doi.org/10.1144/gsjgs.141.3.0555.

[64] Jervey MT. 1988. Quantitative geological modeling of siliciclastic rock sequences and their seismic expression. In: Wilgus, C.K., Hastings, B.S., Kendall, C.G.St.C., Posamentier, H.W., Ross C.A. and Van Wagoner, J.C. (Eds.) Sea Level Changes – An Integrated Approach. Society of Economic Paleontologists and Mineralogists (SEPM), Special Publication 42, 47-69.

[65] Van Wagoner JC, Mitchum Jr RM, Campion KM, Rahmanian VD. 1990. Siliciclastic Sequence Stratigraphy in Well Logs, Core, and Outcrops: Concepts for High-Resolution Correlation of Time and Facies. In: American Association of Petroleum Geologists, Methods in Exploration. Series 7, 55

[66] Catuneanu O. 2006. Principles of Sequence Stratigraphy. Changes, 375. doi:10.5860/Choice.44-4462.

[67] Orton GJ. 1996. Volcanic Environments. Volcanic environments. In: Reading, H.G. (Ed.), Sedimentary Environments: Processes, Facies and Stratigraphy. Blackwell Science, Oxford, pp. 485-567.

[68] Smith GA. 1991. Facies sequences and geometries in continental volcaniclastic sequences in Fisher, R.V., and Smith, G.A., eds., Sedimentation in volcanic settings: SEPM (Society for Sedimentary Geology) Special Publication 45, p. 109-121.

[69] Lucchi F. 2019. On the use of unconformities in volcanic stratigraphy and mapping: Insights from the Aeolian Islands (southern Italy). Journal of Volcanology and Geothermal Research, https://doi.org/10.1016/j.jvolgeores.2019.01.014.

[70] Martí J, Groppelli G, Silveira AB. 2018. Volcanic stratigraphy: A review. Journal of Volcanology and Geothermal Research, 357: 68-91.

[71] Mitchum RM, Vail PR. 1977. Seismic Stratigraphy and Global Changes of Sea Level, Part 7 : Seismic Stratigraphic Interpretation Procedure. Seismic Stratigraphy: Applications

to Hydrocarbon Exploration. AAPG Memoir 26 Memoir 26: 135-43.

[72] de Silva S, Lindsay JM. 2015. Primary Volcanic Landforms. In: H. Sigurdsson (Ed.), The Encyclopedia of Volcanoes (Second Edition), Academic Press, Amsterdam: 273-297. DOI: 10.1016/B978-0-12-385938-9.00015-8.

[73] Holford S, Schofield N, Reynolds P. 2017. Subsurface fluid flow focused by buried volcanoes in sedimentary basins: Evidence from 3D seismic data, Bass Basin, offshore southeastern Australia. 39-50., doi:10.1190/INT-2016-0205.1.

[74] Kumar P, Kamaldeen O, Kalachand S. 2018. Sill Cube: An automated approach for the interpretation of magmatic sill complexes on seismic reflection data. Marine and Petroleum Geology. 100. 10.1016/j.marpetgeo.2018.10.054.

[75] Posamentier HW. 2000. Seismic stratigraphy into the next millennium; a focus on 3D seismic data. American Association of Petroleum Geologists Annual Conference, New Orleans, LA, 16-19

[76] Chopra S, Marfurt KJ. 2005. Seismic Attributes - A Historical Perspective. GEOPHYSICS. doi:10.1190/1.2098670.

[77] Fornaciai A, Favalli M, Karátson D, Tarquini S, Boschi E. 2012. Morphometry of scoria cones, and their relation to geodynamic setting: A DEM-based analysis. J Volcanol Geotherm Res. https://doi.org/10.1016/j.jvolgeores.2011.12.012

[78] Allen JRL. 1983. Studies in Fluviatile Sedimentation: Bars, Bar-Complexes and Sandstone Sheets (Low-Sinuosity Braided Streams) in the Brownstones (L. Devonian), Welsh Borders. Sediment. Geol. 33 (4), 237-93., doi:10.1016/0037-0738(83)90076-3.

[79] Miall AD. 1985. Architectural-Element Analysis: A New Method of Facies Analysis Applied to Fluvial Deposits. Earth Sci. Rev. Elsevier Science Publishers. (BV 22), 261-308., doi:10.1016/0012-8252(85)90001-7

[80] Deptuck ME, Sylvester Z, Pirmez C, O'Byrne C. 2007. Migration – aggradation history and 3-D seismic geomorphology of submarine channels in the Pleistocene Benin-Major Canyon, western Niger delta slope: Marine and Petroleum Geology v. 24, p. 406-433.

[81] Miall AD. 2000. Principles of Sedimentary Basin Analysis; Springer-Verlag, New York, 616p.

[82] Jackson RG. 1975. Hierarchial attributes and a unifying model of bed forms composed of cohesionless material and produced by shearing flow Bull. Geol. Soc. Am., 86 (1975), pp. 1523-1533

[83] White JDL, Valentine GA. 2016. Magmatic versus phreatomagmatic fragmentation: Absence of evidence is not evidence of absence. Geosphere., 2016, https://doi.org/10.1130/GES01337.1

[84] McPhie J, Doyle M, Allen R. 1993. Volcanic textures - a guide to the interpretation of textures in volcanic rocks. Centre for Ore Deposit and Exploration Studies, University of Tasmania

[85] White SM, Crisp JA, Spera FJ. 2006. Long-term volumetric eruption rates and magma budgets. Geochemistry, Geophysics, Geosystems 7(3); doi:10.1029/2005GC001002.

[86] Giba M, Walsh JJ, Nicol A, Mouslopoulou V, Seebeck H. 2013. Investigation of the Spatio-Temporal Relationship between Normal Faulting and Arc Volcanism on Million-Year Time Scales. Journal of the Geological Society 170 (6): 951-62. doi:10.1144/jgs2012-121.

[87] Schofield N, Heaton L, Holford SP, Archer SG, Jackson CAL, Jolley DW. 2012. Seismic imaging of "broken bridges": linking seismic to outcrop-scale investigations of intrusive magma lobes. J Geol Soc. doi:10.1144/0016-76492011-150.

[88] Vries B, Vries M. 2018. Tectonics and Volcanic and Igneous Plumbing Systems. In: Burchardt S (eds) Volcanic and Igneous Plumbing Systems. Elsevier, pp. 111-136. 10.1016/B978-0-12-809749-6.00007-8.

[89] Galland O, Bertelsen HS, Eide CH, Guldstrand F, Haug ØT, Héctor LA, Mair K, Palma O, Planke S, Rabbel O, Rogers B, Schmiedel T, Souche A, Spacapan JB. 2018, Storage and transport of magma in the layered crust-Formation of sills and related float-lying intrusions. In: Burchardt S., (Ed.), Volcanic and Igneous Plumbing Systems, Elsevier. 111-136

[90] Polteau S, Ferré EC, Planke S, Neumann ER, Chevallier L. 2008. How are saucer-shaped sills emplaced? Constraints from the Golden valley sill, South Africa J. Geophys. Res., 113. https://doi.org/10.1029/2008JB005620

[91] Kavanagh JL. 2018. Mechanisms of magma transport in the upper crust – Dyking. In: Volcanic and Igneous Plumbing Systems: Understanding Magma Transport, Storage, and Evolution in the Earth's Crust, S. Burchardt (Ed.), Elsevier. https://doi.org/10.1016/B978-0-12-809749-6.00003-0

[92] Burchardt S, Walter TR, Tuffen H. 2018. Growth of a Volcanic Edifice Through Plumbing System Processes - Volcanic Rift Zones, Magmatic Sheet-Intrusion Swarms and Long-Lived Conduits. In: Burchardt S., (Ed.), Volcanic and Igneous Plumbing Systems, Elsevier. 285-317. https://doi.org/10.1016/B978-0-12-809749-6.00001-7.

[93] Galland O, Spacapan JB, Rabbel O, Mair K, Soto FG, Eiken T, Schiuma M, Leanza HA. 2019. Structure, emplacement mechanism and magma-flow significance of igneous fingers – Implications for sill emplacement in sedimentary basins. Journal of Structural Geology, Volume 124, Pages 120-135. https://doi.org/10.1016/j.jsg.2019.04.013.

[94] Rabbel O, Galland O, Mair K, Lecomte I, Senger K, Spacapan JB, Manceda R. 2018. From field analogues to realistic seismic modelling: a case study of an oil-producing andesitic sill complex in the Neuquén Basin, Argentina. J. Geol. Soc. doi:10.1144/jgs2017-116

[95] Wrona T, Magee C, Fossen H, Gawthorpe RL, Bell RE, Jackson CA-L, Faleide J. 2019. 3-D seismic images of an extensive igneous sill in the lower crust. Geology. 47. DOI: 10.1130/G46150.1

[96] Hansen DM, Cartwright J. 2006. Saucer-Shaped Sill with Lobate Morphology Revealed by 3D Seismic Data: Implications for Resolving a Shallow-Level Sill Emplacement Mechanism. J. Geol. Soc. 163 (3), 509-23., https://doi.org/10.1144/0016-764905-073

[97] Poppe S, Holohan EP, Galland O, Buls N, Gompel G, Keelson B, Tournigand PY, Brancart J, Hollis D, Nila S, Kervyn M. 2019. An inside perspective on magma intrusion: quantifying 3D displacement and strain in laboratory experiments by dynamic X-Ray computed tomography. Front. Earth Sci., 7. https://doi.org/10.3389/feart.2019.00062

[98] Schmiedel T, Kjoberg S, Planke S, Magee C, Galland O, Schofield N, Jackson CAL, Jerram DA. 2017. Mechanisms of overburden deformation associated with the emplacement of the Tulipan sill, mid-Norwegian margin. Interpretation. doi:10.1190/INT-2016-0155.1

[99] Magee C, Murray H, Christopher JAL, Stephen JM. 2019. Burial-Related Compaction Modifies Intrusion-Induced Forced Folds: Implications for Reconciling Roof Uplift Mechanisms Using Seismic Reflection Data. Front Earth Sci. doi:10.3389/feart.2019.00037

[100] Quirie AK, Schofield N, Hartley A, Hole MJ, Archer SG, Underhill JR, Watson D, Holford SP. 2019. The Rattray Volcanics: Mid-Jurassic fissure volcanism in the UK Central North Sea. Journal of the Geological Society, London, 176, 462-481, https://doi.org/10.1144/jgs2018-151

[101] Phillips TB, Magee C, Jackson CAL, Bell RE. 2017. Determining the three-dimensional geometry of a dike swarm and its impact on later rift geometry using seismic reflection data. Geology; 46 (2): 119-122. doi: https://doi.org/10.1130/G39672.1

[102] Valentine GA, Perry FV, Krier D, Keating GN, Kelley RE, Cogbill AH. 2006. Small-volume basaltic volcanoes: eruptive products and processes, and posteruptive geomorphic evolution in Crater Flat (Pleistocene), southern Nevada. Geological Society of America Bulletin 118 (11e12), 1313e1330. http://dx.doi.org/10.1130/B25956.1.

[103] Németh K. 2010. Monogenetic volcanic fields; origin, sedimentary record, and relationship with polygenetic volcanism: Special Paper Geological Society of America, https://doi.org/10.1130/2010.2470(04)

[104] Eichelberger JC, Carrigan C, Westrich HR, Price RH. 1986. Nonexplosive silicic volcanism. Nature Nature 323, 598-602. https://doi.org/10.1038/323598a0

[105] Kósik S, Németh K, Lexa J, Procter J. 2019. Understanding the evolution of a small-volume silicic fissure eruption: Puketerata Volcanic Complex, Taupo Volcanic Zone, New Zealand. Journal of Volcanology and Geothermal Research. 383. 28-46. 10.1016/j.jvolgeores.2017.12.008.

[106] Vespermann D, Schminke H-U. 2000. Scoria cones and tuff rings. In: Sigurdsson,H., Houghton, B.F., McNutt, S.R., Rymer,H., Stix, J. (Eds.), Encyclopedia of Volcanoes. Academic Press, San Diego, pp. 683e694.

[107] Lorenz V. 1985. Maars and diatremes of phreatomagmatic origin, a review. T. Geol. Soc. South Africa. 88, 459-470.

[108] Svensen H, Planke S, Malthe-Sorenssen A, Jamtveit B, Myklebust R, Eidem TR, Rey SS. 2004. Release of methane from a volcanic basin as a mechanism for initial Eocene global warming. Nature. 429, 542-545

[109] White JDL, Ross PS. 2011. Maar-diatreme volcanoes: A review. https://doi.org/10.1016/j.jvolgeores.2011.01.010

[110] Kjoberg S, Schmiedel T, Planke S, Svensen HH, Millett JM, Jerram DA, Galland O, et al. 2017. 3D structure and formation of hydrothermal vent complexes at the Paleocene-Eocene transition, the Møre Basin, mid-Norwegian margin. Interpretation 5: SK65-SK81. https://doi.org/10.1190/INT-2016-0159.1

[111] Aarnes I, Planke S, Trulsvik M, Svensen H. 2015. Contact metamorphism and thermogenic gas generation in the Vøring and Møre basins, offshore Norway, during the Paleocene-Eocene thermal maximum. J Geol Soc 172: 588-598

[112] Davidson JP, de Silva SL, 2000. Composite volcanoes. In: Sigurdsson,H., Houghton, B.F.,McNutt, S.R., Rymer, H., Stix, J. (Eds.), Encyclopedia of Volcanoes. Academic Press, San Diego, pp. 663e680.

[113] Hackett WR, Houghton BF. 1989. A facies model for a quaternary andesitic composite volcano: Ruapehu, New

Zealand. Bulletin of Volcanology 51, 51e68.

[114] Cotton CA. 1944. Volcanoes as Landscape Forms. Whitcombe and Tombs, Christchurch, New Zealand.

[115] Moore JG, Clague DA. 1992. Volcano growth and evolution of the island of Hawaii, Geol. Soc. Am. Bull., 104, 1471–1484. https://doi.org/10.1130/0016-7606(1992)104<1471:VGAEOT>2.3.CO;2

[116] Walker GPL. 2000. Basaltic volcanoes and volcanic systems. In: Sigurdsson, H., Houghton, B.F., McNutt, S.R., Rymer, H., Stix, J. (Eds.), Encyclopedia of Volcanoes, first ed. Academic Press, San Diego, pp. 283e290.

[117] Skilling IP. 2002. Basaltic pahoehoe lava-fed deltas: Largescale characteristics, clast generation, emplacement processes and environmental discrimination: Geological Society, London, Special Publications 202, 91-113. https://doi.org/10.1144/GSL.SP.2002.202.01.06

[118] Morley C. 2018. 3D seismic imaging of the plumbing system of the Kora volcano, Taranaki Basin, New Zealand: The influences of syn-rift structure on shallow igneous intrusion architecture: Geosphere, 2018. doi.org/10.1130/GES01645.1.

[119] Kennedy BM, Holohan EP, Stix J, Gravley DM, Davidson JRJ, Cole JW, Burchardt S. 2018. Volcanic and Igneous Plumbing Systems of Caldera Volcanoes. In: Volcanic and Igneous Plumbing Systems: Understanding Magma Transport, Storage, and Evolution in the Earth's Crust, S. Burchardt (Ed.), Elsevier. https://doi.org/10.1016/B978-0-12-809749-6.00010-8.

[120] Cole JW, Milner DM, Spinks KD. 2005. Calderas and caldera structures: a review. Earth-Science Reviews 69 (1e2), 1e26.

[121] Wilson CJN, Houghton BF, McWilliams MO, Lanphere MA, Weaver SD, Briggs RM. 1995. Volcanic and structural evolution of Taupo Volcanic Zone, New Zealand: a review. Journal of Volcanology and Geothermal Research 68, 1e28.

[122] Martí J, Geyer A, Folch A, Gottsmann J. 2008. A review on collapse caldera modelling. In Caldera Volcanism: Analysis, Modelling and Response, eds J. Gottsmann and J. Martí (Amsterdam: Elsevier), 233-283.

[123] Lipman PW. 2000. Calderas. In: Sigurdsson, H., Houghton, B.F., McNutt, S.R., Rymer, H., Stix, J. (Eds.), Encyclopedia of Volcanoes. Academic Press, San Diego.

[124] Branney M, Acocella V. 2015. Calderas. in The Encyclopaedia of Volcanoes, eds H. Sigurdsson, B. Houghton, H. Rymer, and J. Stix (Cambridge: Academic Press).

[125] Coffin MF, Eldholm O. 1993. Large igneous provinces. Scientific American. ISSN: 0036-8733 269 (4), 42e49.

[126] Self S, Thordarson T, Keszthelyi L. 1997. Emplacement of continental flood basalt lava flows. In: Large Igneous Provinces: Continental, Oceanic, and Planetary Flood Volcanism, pp. 381e410.

[127] Sheth H. 2007. Large Igneous Provinces (LIPs): Definition, recommended terminology, and a hierarchical classification. Earth-Science Reviews. 85. 10.1016. DOI: 10.1016/j.earscirev.2007.07.005

[128] Single RT, Jerram DA. 2004. The 3D facies architecture of flood basalt provinces and their internal heterogeneity: Examples from the Palaeogene Skye Lava Field: Journal of the Geological Society, 161, 911-926, doi: 10.1144/0016-764903-136.

[129] Thordarson T, Self S. 1993. The Laki (Skaftár Fires) and Grímsvötn

eruptions in 1783-1785. Bulletin of Volcanology 55:233-263. DOI: 10.1007/BF00624353

[130] Jerram DA. Volcanology and facies architecture of flood basalts. In: Menzies MA, Klemperer SL, Ebinger CJ, Baker J, editors. Magmatic riftedmargins: Geological society of america special paper. 2002;362:119-132.

[131] Rey SS, Planke S, Symonds PA, Faleide JI. 2008. Seismic volcano-stratigraphy of the Gascoyne margin, Western Australia, J. Volcanol. Geotherm. Res., 172(1-2), 112-131, doi:10.1016/j.jvolgeores.2006.11.013.

[132] Wright KA, Davies RJ, Jerram DA, Morris J, Fletcher R. 2012. Application of seismic and sequence stratigraphic concepts to a lava-fed delta system in the Faroe-Shetland Basin, UK and Faroes: Basin Research, 24, 91-106, doi: 10.1111/j.1365-2117.2011.00513.x.

[133] Watton TJ, Jerram DA, Thordarson T, Davies RJ. 2013. Three-dimensional lithofacies variations in hyaloclastite deposits: Journal of Volcanology and Geothermal Research, 250, 19-33, doi: 10.1016/j.jvolgeores.2012.10.011.

[134] Cannon EC, Bürgmann R. Prehistoric fault offsets of the Hilina fault system, south flank of Kilauea Volcano, Hawaii: Journal of Geophysical Research; 2001;106:4207-4219. DOI: 10.1029/2000JB900412.